IEEE Access
Multidisciplinary | Rapid Review | Open Access Journal

Received June 10, 2020, accepted June 22, 2020, date of publication July 3, 2020, date of current version July 15, 2020.

Digital Object Identifier 10.1109/ACCESS.2020.3007022

Offline Selective Harmonic Elimination With (2*N*+1) Output Voltage Levels in Modular Multilevel Converter Using a Differential Harmony Search Algorithm

YAYUN XIN[1], JIN YI[2], KAI ZHANG[1], CANFENG CHEN[1], AND JIAN XIONG[1]

[1]Department of Applied Electronic Engineering, School of Electrical and Electronic Engineering, Huazhong University of Science and Technology, Wuhan 430074, China

[2]Environmental Research Institute, National University of Singapore, Singapore 119077

Corresponding author: Jin Yi (yijinbike@gmail.com)

This work was supported by the National Science Foundation of China under Grant 51477063.

ABSTRACT (2*N*+1) selective harmonic elimination pulse-width modulation (SHE-PWM) is an effective switching strategy of the modular multilevel converter in medium-voltage cases. In these cases, the number of sub-modules (SMs) is not high. Compared to the traditional (*N*+1) SHE-PWM, (2*N*+1) SHE-PWM has *N* more voltage levels, thus it can yield much better harmonic performance. However, the task of selective harmonic elimination also becomes much more complicated since there are more switching angles to be determined. This paper proposes a differential harmony search algorithm (DHS) with a novel harmony improvisation procedure for solving this problem. The Bayesian optimization method is applied to find the optimal parameter configuration for DHS. The performance of DHS is compared with 6 other metaheuristic algorithms including differential evolution (DE), harmony search (HS), genetic algorithm (GA), particle swarm optimization (PSO), teaching and learning-based optimization (TLBO), and ant colony optimization (ACO). The comparison is conducted on a set of 100 (2*N* +1) SHE-PWM instances by varying the modulation index from 0.01 to 1.0 with a step of 0.01. The numerical results show that the proposed DHS outperforms other compared methods in terms of objective function values, algorithm robustness, the magnitude of fundamental harmonic, and the calculated total harmonic distortion values. The switching angles obtained by DHS are further validated by both Matlab/Simulink simulation and hardware experiment.

INDEX TERMS (2*N*+1) SHE-PWM, modular multilevel converter, harmony search algorithm.

NOMENCLATURE

ACO	Ant colony optimization
CDF	Cumulative distribution function
DE	Differential evolution
DHS	Differential harmony search
GA	Genetic algorithm
HS	Harmony search
HVDC	High voltage direct current
ICA	Imperialist competitive algorithm
MMC	Modular multilevel converter
MVAC	Medium voltage AC
PSO	Particle swarm optimization
SHE-PWM	Selective harmonic elimination pulse-width modulation
SM	Sub-module
TLBO	Teaching and learning-based optimization
M	Modulation index
N	Number of sub-modules in each arm
N_{lower}	Number of sub-module installations in lower arm
N_{upper}	Number of sub-module installations in upper arm
V_{dc}	DC source voltage value
v_{uN}	Output voltage of phase u
ω	Radius speed
b_{h_s}	The h_s th order harmonic amplitude

The associate editor coordinating the review of this manuscript and approving it for publication was Yijie Wang.

l	Total number of switching angles in the first quarter-waveform
m_k	A sign function that outputs positive or negative step depending on corresponding θ_k
$\boldsymbol{\theta}$	A set of switching angles i.e., $\boldsymbol{\theta} = (\theta_1, \theta_2, ..., \theta_l)$
$\boldsymbol{\alpha}$	A set of firing angles i.e., $\boldsymbol{\alpha} = (\alpha_1, \alpha_2, ..., \alpha_l)$
θ_k	The k th switching angle in the first quarter-waveform
α_k	The k th firing angle in the first quarter-waveform
V_1	The actual amplitude of the fundamental component normalized by V_{dc}
$V_1{}^*$	The desired set amplitude of the fundamental component normalized by V_{dc}
h_s	The s th non-triple odd harmonic i.e., the h_s th harmonic
Har	The total number of harmonics (the fundamental harmonic and other low-order harmonics) to be handled, and $Har = 17$
V_{h_s}	The amplitude of the h_s th harmonic component normalized by V_{dc}
ϕ	The penalty function factor
$g_i(\boldsymbol{\alpha})$	Constraint function in optimization model
$S_j(\boldsymbol{\alpha})$	A threshold function representing the current switching angle value compared to $\pi/2$
$L_i(\boldsymbol{\alpha})$	The level of waveform, i.e. a cumulative $S_j(\boldsymbol{\alpha})$ from $j = 1$ to $j = i$
HMS	The size of the harmony memory pool in the harmony search algorithm
$HMCR$	The harmony memory consideration rate
PAR	The pitch adjustment rate
BW	The distance bandwidth
$maxFEs$	The maximum number of function evaluations
FEs	The current number of function evaluations

I. INTRODUCTION

The MMC is one of the most promising multi-level converter topologies which was first introduced by Lesnicar and Marquardt [1]. A typical half-bridge SM based circuit topology of MMC is depicted in Fig. 1.

Nowadays, MMC not only has been widely used in HVDC systems [2], [3], but also in various medium-voltage applications such as battery energy storage [4], medium voltage motor drives [5], MVAC distribution network [6], because of its high-quality output waveform, fewer converter losses, and modularity of structure [7].

In medium-voltage cases, the SHE-PWM is widely used and studied, due to its lower switching losses and tight control of low-order harmonics. In [8], a (2*N*+1) SHE-PWM was proposed and firstly put into practical application (*N* represents the number of sub-modules in each arm).

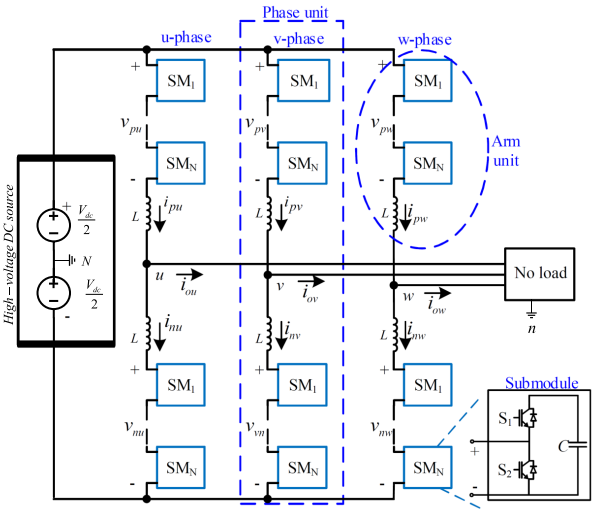

FIGURE 1. Typical circuit topology of three-phase MMC.

It has *N* more output voltage levels compared with (*N*+1) SHE-PWM. Given the same number of SMs and switching frequency, (2*N*+1) SHE-PWM has *N* more firing angles over the fundamental period and can control twice as many harmonics as (*N*+1) SHE-PWM. As a result, (2*N*+1) SHE-PWM is regarded as a promising SHE-PWM, and more details about the studies on (2*N*+1) SHE-PWM can be found in [9], [10].

To yield good harmonic performance in MMC with SHE-PWM, the harmonic contents of a PWM waveform are mathematically expressed by a group of nonlinear and transcendental switching angle equations, and their solution can be found by many ever proposed different approaches. Numerical approaches such as the Newton-Raphson method was firstly utilized in [11]. However, its performance heavily relies on the starting point and it cannot find multiple solutions [12]. Walsh functions can convert the equations into a set of linear algebraic equations [13], but its accuracy depends on the sampling points [12]. Thus the higher accuracy is required, and much more computational resources will be consumed. Some methods transformed the trigonometric equations into an equivalent set of polynomial equations [14]. However, if many orders of harmonics need to be eliminated, the order of polynomials increases accordingly [12], which makes the equations much more difficult to solve. Some other methods that facilitate online implementation were recently proposed [15], [16], but they need more advanced computing powers and memory capabilities [12].

To overcome the disadvantages of the aforementioned methods and guarantee the accuracy of (2*N*+1) SHE-PWM, the corresponding transcendental equations can be reformulated into an optimization problem. In the optimization model, trigonometric equations for each harmonic are represented in a cost function, in which the fundamental harmonic is controlled to approach the predefined value as much as possible, while other odd non-triple-order harmonics are eliminated to zero [8], [10].

In recent years, meta-heuristic algorithms have been widely adopted to solve engineering optimization problems because of their advantages such as easy to understand and implement, computationally efficient, and no need for prior knowledge on the objective functions. The meta-heuristic algorithms also have been used to solve the SHE-PWM problems, which include GA [17], PSO [18], TLBO [19]. There are also several papers that provided some comparative studies among different meta-heuristic algorithms on SHE-PWM. For example, Etesami *et al.* [20] compared the imperialist competitive algorithm (ICA) with PSO on solving the SHE-PWM and the modified SHE-PWM problem. Memon *et al.* [21] compared several bio-inspired meta-heuristic algorithms such as GA, PSO, and DE on SHE-PWM problem for renewable energy conversion applications. Both of the comparative studies above were conducted on the $(N+1)$ SHE-PWM, and the numbers of switching angles are relatively small (the numbers of switching angles considered in the above two studies are only 5 and 3). However, in $(2N+1)$ SHE-PWM there are N more levels which result in much more switching angle variables (17 in this study) and therefore a much more complicated optimization problem.

The harmony search (HS) algorithm is a metaheuristic optimization method inspired by the instrument playing process in which the musicians continuously adjust the pitch of their instruments to get better harmony [22]–[24]. The global optimization process is very similar to the instrument playing process, where each decision variable continuously changes its value during the search process and converges to the global optimum. HS is simple in concept, easy in implementation with few parameters [25]. Since it was first introduced in 2001, HS has caught a lot of researchers' attention and been widely applied to various disciplines which also include the field of electrical and power system, such as electrical distribution network reconfiguration [26], optimal placement of distributed generators in distribution systems [27], controller parameters optimization of distributed-generation system [28], and combined economic emission dispatch problem [29]. More detailed reviews on the HS algorithms and their applications to solve problems in the electrical power system area can be found in [30]–[32].

In this paper, an improved version of the HS algorithm called differential harmony search (DHS) algorithm is proposed to solve the $(2N+1)$ SHE-PWM. DHS adopts novel improvisation and pitch adjustment procedures and it's more efficient than HS. Besides, the Bayesian optimization method is applied to find the optimal parameter configuration for DHS. The performance of DHS is compared with other 6 metaheuristic algorithms including DE, HS, GA, PSO, ACO, and TLBO on 100 $(2N+1)$ SHE-PWM problem instances with different modulation indexes. These algorithms are critically evaluated in terms of objective function values, algorithm robustness, the magnitude of fundamental harmonic, and the calculated THD values. The numerical results show the superior performance of DHS to other algorithms. The switching angles obtained by DHS are further validated by both simulation and hardware experiments, which demonstrates the capability of DHS in practical use.

As it's highlighted in the title, our proposed approach is an offline strategy. In our approach, all the switching angles are calculated by DHS first, then these switching angles are saved in a look-up table and then copied to the board. During the real-time control process, the switching angles are read directly from the look-up table. The reason for using the offline mode is that the optimization process is time-consuming (i.e, seconds), but in the real-time control process, we need to find a set of switching angles within 0.02s (50Hz). It's impractical to run an optimization algorithm directly on the board.

The contributions of this paper can be summarized as follows.

(1) A new formulation with a few constraints is built for the $(2N+1)$ SHE-PWM problem.
(2) To solve the $(2N+1)$ SHE-PWM, a novel differential harmony search algorithm is proposed, and the Bayesian optimization-based automatic parameter tuning procedure is applied to find the optimal parameter configurations.
(3) Empirically, we demonstrate that the proposed DHS algorithm outperforms 6 other well-known meta-heuristic algorithms on 100 $(2N+1)$ SHE-PWM instances. Besides, both the simulation and hardware experiment results validate the effectiveness of DHS and confirm its capability in practical use.

The remaining of this paper is organized as follows. The formulation and operation principles of MMC to solve the $(2N+1)$ SHE-PWM problem are described in Section II. Section III introduces the proposed DHS. Section IV provides numerical and simulation results. Section V presents the hardware experiment results. Finally, section VI gives the concluding remarks.

II. FORMULATION OF (2N+1) SHE-PWM

A typical circuit topology of the three-phase MMC arming N SMs is shown in Fig. 1. We assume that the phase output voltage v_{uN} is formulated as

$$v_{uN} = \frac{MV_{dc}}{2}\sin(\omega t) \tag{1}$$

where M is the modulation index.

For $(2N+1)$ SHE-PWM, it has N more output voltage levels than traditional $(N+1)$ SHE-PWM. Taking $N = 4$ as an example, because the output phase voltage $v_{uN} = (N_{lower} - N_{upper})/2 \cdot V_{dc}/4$, the additional 4 levels are acquired by inserting some time fragments of 5 or 3 installations among those of 4 installations in the same leg during the fundamental period, as shown in Fig. 2. And the detailed upper and lower arm installations in the same leg to output all the 9 phase voltage levels are depicted in Fig. 2, in which the SMs shaded by blue block are installations.

Typical first quarter and all quarters of the output phase voltage waveform are depicted in Fig. 3. Based on the features

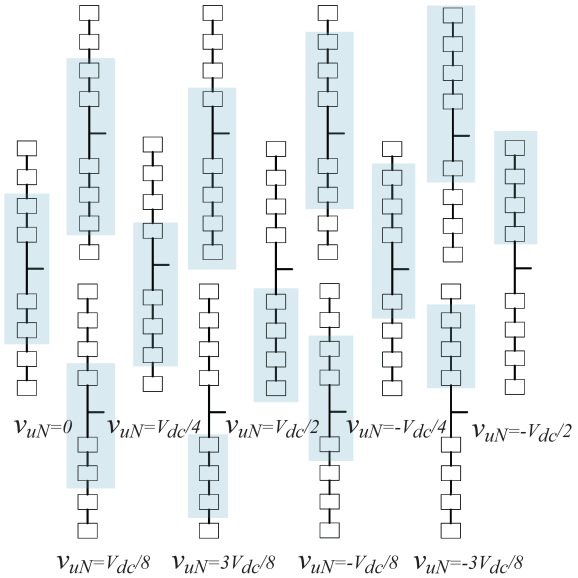

FIGURE 2. The detailed installations in the same leg to acquire 9 output phase voltage levels when $N = 4$.

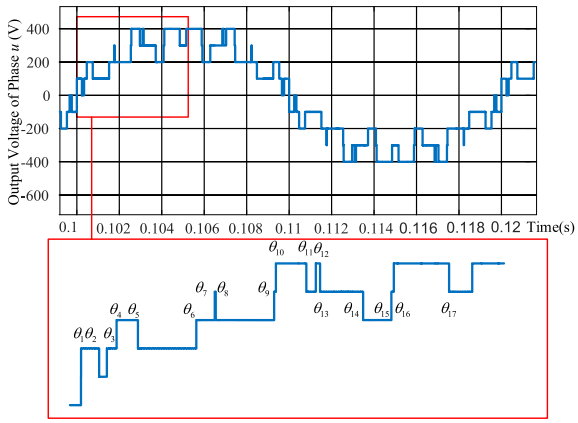

FIGURE 3. The first quarter and all quarters of output phase voltage waveform.

of three-phase symmetrical prototype, and the requirements of line voltage harmonic elimination, non-triple odd harmonics are only taken into consideration to eliminate. And thus the phase output voltage can be expressed as Fourier expression (2), where b_{h_s} can be derived in (3). In (3), and θ_k meets the demand of (5) [10], [33].

$$v_{uN} = \sum_{h_s=1,5,7,\ldots}^{\infty} b_{h_s} \sin(h_s \omega t) \tag{2}$$

$$b_{h_s} = \frac{2V_{dc}}{h_s \pi N} \sum_{k=1}^{l} m_k \cos(h_s \theta_k) \tag{3}$$

$$m_k = \begin{cases} 1, & \text{when } \theta_k \text{ is the positive step;} \\ -1, & \text{when } \theta_k \text{ is the negative step.} \end{cases} \tag{4}$$

$$0 < \theta_1 < \theta_2 < \theta_3 < \cdots < \theta_l < \frac{\pi}{2} \tag{5}$$

Due to the odd symmetry characteristic of the *cos* function within the domain of $(0, \pi)$, the expression of b_{h_s} can be simplified by introducing a set of firing angles $\boldsymbol{\alpha} = (\alpha_1, \alpha_2, \ldots, \alpha_l)$ corresponding to the switching angles $\boldsymbol{\theta} = (\theta_1, \theta_2, \ldots, \theta_l)$:

$$\theta_k = \begin{cases} \alpha_k, & \alpha_k \le \pi/2 \\ \pi - \alpha_k, & \alpha_k > \pi/2 \end{cases} \tag{6}$$

To offer tight control of required low-order harmonics, omitting triplen harmonics regarding a three-phase MMC, a generalized optimization model thus can be formulated as [34], [35]:

$$Min : F(\boldsymbol{\alpha}) = (10\frac{V_1^* - V_1}{V_1^*})^4 + \sum_{s=2}^{Har} \frac{1}{h_s}(50\frac{V_{h_s}}{V_1})^2 \tag{7a}$$

$$subject\ to : \begin{cases} 0 \le \alpha_i \le \pi, 1 \le i \le l \\ g_j(\boldsymbol{\alpha}) = L_j(\boldsymbol{\alpha}) - N \le 0, 1 \le j \le l \\ g_k(\boldsymbol{\alpha}) = -L_k(\boldsymbol{\alpha}) \le 0, l+1 \le k \le 2*l \\ g_{2*l+1}(\boldsymbol{\alpha}) = abs(l - len(unique(\boldsymbol{\alpha}))) = 0 \end{cases} \tag{7b}$$

$$L_i(\boldsymbol{\alpha}) = \sum_{j=1}^{i} S_j(\boldsymbol{\alpha}), 1 \le i \le 2*l \tag{8}$$

$$S_j(\boldsymbol{\alpha}) = \begin{cases} 1, & \alpha_j \le \pi/2 \\ -1, & \alpha_j > \pi/2 \end{cases} \tag{9}$$

where V_1^* is set to $M/2$ in our study as shown in (10). *Har* equals to 17 in this study, and $h_2 = 5, h_3 = 7, \ldots, h_{17} = 49$. The expressions of V_{h_s} are given in (10)-(12). The first aim is to strictly control the magnitude of the fundamental harmonic and follow its desirable value. Different from previous settings, we allow higher deviation on the magnitude of the fundamental harmonic. The reason is that in various engineering applications, higher waveform quality of the output signal may be achieved with some extent of sacrifices on the precision in terms of the magnitude of the fundamental harmonic [20]. In this regard, a penalty is activated when the deviation on the magnitude of the fundamental harmonic is higher than 10%, which is expressed in the first term of (7a). The second term of (7a) maintains target harmonics below 2% of the fundamental component to respect the IEEE-519 standard (<3%) [36]. $\boldsymbol{\alpha} = (\alpha_1, \alpha_2, \ldots, \alpha_l)$ is the decision variables consist of a set of firing angles corresponding to switching angle $\boldsymbol{\theta} = (\theta_1, \theta_2, \ldots, \theta_l)$ satisfying (6). In addition, the objective function is subjected to several constraints satisfying (7b), i.e. (1) the firing angles should be within the range of $(0, \pi)$; (2) the levels of waveform $L_i(\boldsymbol{\alpha})$ should be in the range of minimum and maximum allowed levels in the first half waveform; (3) all the switching angles $\boldsymbol{\theta}$ should be unique with each other.

$$V_1 = \frac{2}{\pi N}(\cos(\alpha_1) + \cos(\alpha_2) + \cdots + \cos(\alpha_l)) = M/2 \tag{10}$$

$$V_5 = \frac{2}{5\pi N}(\cos(5\alpha_1) + \cos(5\alpha_2) + \cdots + \cos(5\alpha_l)) \tag{11}$$

$$V_{h_s} = \frac{2}{h_s \pi N}(\cos(h_s\alpha_1)+\cos(h_s\alpha_2)+\cdots+\cos(h_s\alpha_l)) \quad (12)$$

$$0 \le M \le 1 \quad (13)$$

With the help of the penalty function method [37], the objective function can be re-formulated as:

$$Min: F(\boldsymbol{\alpha}) = (10\frac{V_1^* - V_1}{V_1^*})^4 + \sum_{s=2}^{Har}\frac{1}{h_s}(50\frac{V_{h_s}}{V_1})^2 + \phi \cdot \sum_{i=1}^{2*l+1} max\{0, g_i(\boldsymbol{\alpha})\} \quad (14)$$

where the last part of the objective function is the penalty function of the constraint violations, and ϕ is set to 10^6 based on empirical experience.

It can be seen from the objective function that it's a nonlinear optimization problem with 17 decision variables. In practical use, the optimization methods are needed to run multiple trials over a range of M values within the domain of (0, 1]. Therefore, an efficient optimization algorithm is in great demand. In the next section, DHS will be developed to solve this problem.

III. PROPOSED OPTIMIZATION APPROACH

A. HARMONY SEARCH ALGORITHM

The whole working process of HS for solving an optimization problem can be divided into five main steps. Let $f(\boldsymbol{x})$ be the targeted minimization problem, $\boldsymbol{x} = (x_1, x_2, \cdots, x_d)$ is the decision vector, d is the number of decision variables, and x_i $(1 \le i \le d)$ is the i-th decision variable. L_i and U_i are the lower and upper bounds on x_i $(L_i \le x_i \le U_i)$. The working steps of HS to find the optimal solution for $f(\boldsymbol{x})$ can be summarized as:

Step 1: Define the parameters in HS. These parameters are: the harmony memory size (*HMS*), or the number of solution vectors in the harmony memory; harmony memory considering rate (*HMCR*); pitch adjusting rate (*PAR*); distance bandwidth(*BW*); the maximum number of function evaluations (*maxFEs*).

Step 2: Initialize the harmony memory (HM). Randomly generate *HMS* solutions within the domain and store them in HM by using (15).

$$x_{i,j} = L_j + rand \cdot (U_j - L_j) \quad (15)$$

where $i = 1, 2, \cdots, HMS, j = 1, 2, \cdots, d$, *rand* is a random number in range of (0, 1).

Step 3: When the HM is initialized, a new candidate harmony is improvised by following three rules: (1) randomly pick a value from all of the solutions in the HM with a memory consideration rate (*HMCR*), (2) this value can be further adjusted with a pitch adjustment rate (*PAR*) (3) a random re-initialization procedure with probability of $(1 - HMCR)$. The detail of the new harmony improvisation steps is summarized in Algorithm 1.

Step 4: Update the solutions in HM. In this step, the new improvised harmony is first evaluated by the objective function ($f(\boldsymbol{x})$) and then compare with the fitness value of the worst harmony from the current HM. If the objective function of the new harmony is equal to or better than the worst harmony in the current HM, then the worst harmony will be replaced by the new harmony; otherwise, the harmony individuals in the current HM remain the same.

Step 5: Checking the stopping criterion. The HS algorithm will stop the iteration and output the best solution found so far if the current iteration number reaches *maxFEs*; otherwise, repeat the procedures from Step 3-4.

Algorithm 1 Improvisation of New Harmony in HS Algorithm

```
for j = 1 to d do
  if rand < HMCR then
    new_x_j = x_{a,j}, a ∈ {1, 2, ..., HMS} /*Choose a value from HM on dimension j*/
    if rand < PAR then
      new_x_j = new_x_j ± rand · BW /*Pitch adjustment */
    end if
  else
    new_x_j = L_j + rand · (U_j − L_j) /*Randomly generate a value */
  end if
end for
```

B. DIFFERENTIAL EVOLUTION

The differential evolution (DE) algorithm is a population-based global optimizer and it was first proposed by Storn and Price [38]. DE shows its superiority over many optimization methods in terms of solution accuracy, convergence speed, and robustness. The original DE is known as *DE/rand/1*, while there are several other DE variants with different mutation strategies, such as *DE/best/1*, *DE/best/2*, *DE/current-best/1* and *DE/current-best/2*.

Suppose there is DE population P, and x_{best} denotes the best individual among P. Let $x = (x_1, \cdots, x_d) \in \mathbb{R}^d$ be an individual solution in P. There are several ways to generate a child individual $u = (u^1, \cdots, u^d) \in \mathbb{R}^d$ based on different mutation strategies. First we need to obtain the donor vector v_i by mutation, which has the following forms:

(1) DE/rand/1:

$$v_i = x_{r_1} + F \cdot (x_{r_2} - x_{r_3}) \quad (16)$$

(2) DE/best/1:

$$v_i = x_{best} + F \cdot (x_{r_1} - x_{r_2}) \quad (17)$$

(3) DE/best/2:

$$v_i = x_{best} + F \cdot (x_{r_1} - x_{r_2}) + F \cdot (x_{r_3} - x_{r_4}) \quad (18)$$

(4) DE/current-best/1:

$$v_i = x_i + F \cdot (x_{r_1} - x_{r_2}) \quad (19)$$

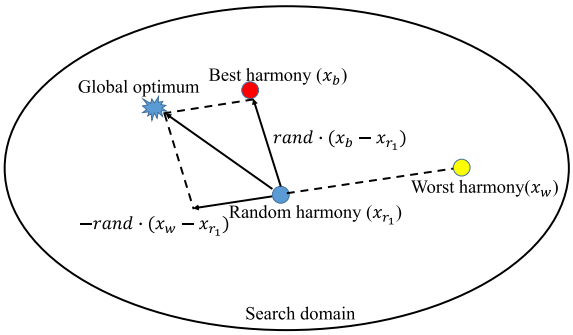

FIGURE 4. Illustration of the learning process within the memory consideration phase in DHS.

(5) DE/current-best/2:

$$v_i = x_i + F \cdot (x_{r_1} - x_{r_2}) + F \cdot (x_{r_3} - x_{r_4}) \tag{20}$$

After the mutation operation, the next step is to produce the child solution u using crossover operation between v_i and x_i with a crossover rate of $CR \in [0, 1]$ [38].

C. PROPOSED DIFFERENTIAL HARMONY SEARCH ALGORITHM FOR SHE-PWM

Although the basic HS algorithm can quickly identify the high-performance regions of the search, it is not efficient in performing local search and refine the final solutions [39]. Besides, the performance of HS is highly reliant on its control parameters. However, parameter tuning is a challenging task. For example, the *bw* parameter defines the pitch adjustment step, a larger value will encourage exploration and a smaller value will encourage exploitation, and proper *bw* value is also problem-independent. Most previous studies dynamically change the value of *bw* based on the optimization process, but the initial *bw* value still needs to be defined. To eliminate the parameter of *bw* and to improve the solution accuracy of HS, a differential harmony search (DHS) is proposed. The details of DHS are given below.

During the memory consideration phase of HS, the value of new harmony only learns from harmonies in the current HM. To avoid the premature of HS, we add extra shifts to the new harmony. The basic idea behind is that the new harmony not only trying to move towards the direction of the best harmony in the current HM but also trying to avoid not moving close to the worst harmony in the current HM (see Fig. 4). The new harmony memory consideration procedure is shown as:

$$new\_x_j = x_{r_1,j} + rand \cdot (x_{b,j} - x_{r_1,j}) - rand \cdot (x_{w,j} - x_{r_1,j}), \tag{21}$$

In our proposed DHS, the pitch adjustment method of conventional HS is replaced by the "DE/best/1" mutation operation. In the new pitch adjustment procedure, the new harmony is perturbing around the current best harmony with a step determined by the distance between two random picked harmony individuals. The new pitch adjustment procedure is shown as:

$$new\_x_j = x_{b,j} + rand \cdot (x_{r_2,j} - x_{r_3,j}),\ r_2 \neq r_3 \tag{22}$$

The new pitch adjustment method eliminated the need for using *bw*, which lightens the human effort for parameter tuning. Besides, the use of distances between two harmony individuals as the adjustment step makes the DHS algorithm much easier adapting to different problems, and it also makes the algorithm effective in both global and local searches. The detail of the new harmony improvisation steps in DHS algorithm is summarized in Algorithm 2.

Algorithm 2 Improvisation of New Harmony in DHS Algorithm

```
for j = 1 to d do
  if rand < HMCR then
    new_x_j = x_{r1,j} + rand·(x_{b,j} − x_{r1,j}) − rand·(x_{w,j} − x_{r1,j}),
    r1 ∈ {1, 2, ..., HMS} /*Choose a value from HM on
    dimension j*/
    if rand < PAR then
      new_x_j = x_{b,j} + rand · (x_{r2,j} − x_{r3,j}) /*Pitch adjust-
      ment */
    end if
  else
    new_x_j = L_j + rand · (U_j − L_j) /*Randomly generate
    a value */
  end if
end for
```

The computational procedure of DHS for solving the (2*N*+1) SHE-PWM problem is shown in Fig. 5.

IV. NUMERICAL AND SIMULATION RESULTS

In this section, the effectiveness of our proposed DHS is validated on a set of (2*N*+1) SHE-PWM problems and compared with other widely used metaheuristic algorithms including GA, PSO, DE, ACO, BA, TLBO, and HS. Then, a Matlab/Simulink model of a three-phase MMC is developed to validate the numerical results. All the numerical experiments are implemented on a desktop computer with an Intel 3.3GHz i5-2500 CPU, 8G RAM and IDE of Matlab 2018b.

A. EXPERIMENT SETUP FOR NUMERICAL COMPARISON

In this experiment, a set of 100 different (2*N*+1) SHE-PWM problem instances with the modulation index varying from 0.01 to 1.0 are used to validate the performance of the compared methods. For this aim, the mathematical formulation introduced in section II is adopted. All compared algorithms perform 30 independent trials on each of the problems, and for each single run, the maximum number of function evaluations (*maxFEs*) is set to 50000. The parameter settings for the compared methods are shown in Table 1, which are following the recommendation from previous studies [19].

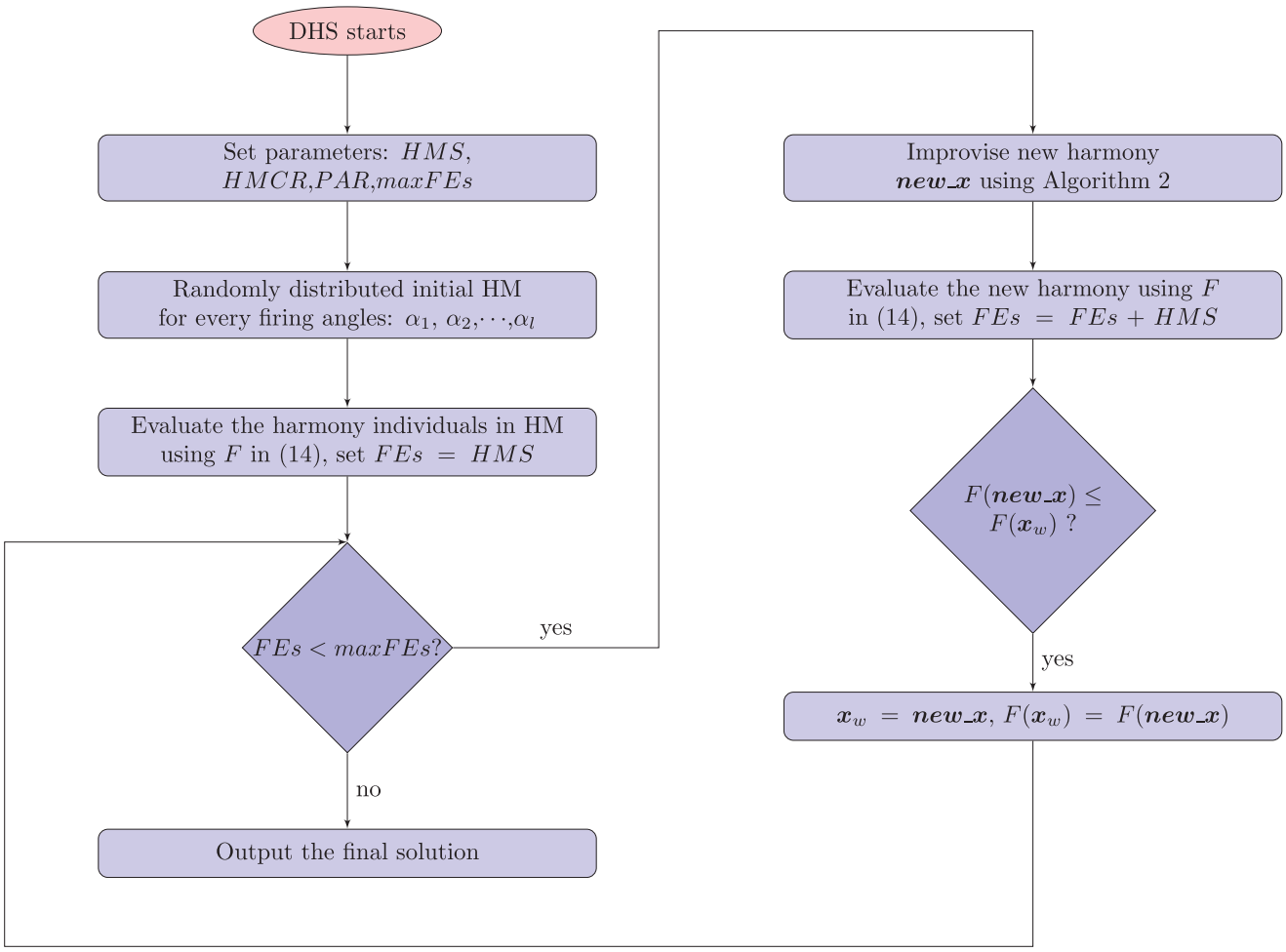

FIGURE 5. The flowchart of DHS for solving the SHE-PWM problem.

B. AUTOMATIC PARAMETER CONFIGURATION USING BAYESIAN OPTIMIZATION

As mentioned above, the performance of HS is sensitive to its parameters, a better parameter configuration may contribute to significant improvement in solution quality. However, searching for an optimal parameter configuration for HS is a challenging task. Many previous studies have discussed this topic. In some previous studies [40], [41], the authors tried to find the best HS parameters by independently adjusting only one factor at a time. Other methods like experiment design method were also applied. For example, Jin *et al.* [42] applied the Orthogonal experiment design to search for optimal HS parameters. The shortcomings of these methods are twofold: firstly, the obtained parameter configuration may not be the best because they only explored in a small subspace; Secondly, most of these methods have huge human labor involved.

In this study, we adopt an automatic parameter configuration procedure. First, the search for optimal parameter configuration is formulated as an optimization problem, in which the objective function is the overall performance on all test problems (the formulation can be found in Appendix A). Then the optimal parameter configuration can be automatically obtained by an optimization algorithm. Since the evaluation process of the parameter configuration is time-consuming (minutes for a single run), we adopt the Bayesian optimization method [43] to solve this problem. The Bayesian optimization is an efficient approach to optimizing objective functions that are computationally-expensive (minutes or hours). It first builds a surrogate model for the objective function and quantifies the uncertainty in that surrogate using a Gaussian process regression, and then uses an acquisition function defined from this surrogate to decide where to sample. We stop the Bayesian optimization method after 50 iterations, and obtain the parameter configurations: $HMS = 50$, $HMCR = 0.999$, $PAR = 0.8627$. The progress plot of the Bayesian optimization is depicted in Fig. 6.

C. COMPARISON ON COMPUTATIONAL RESULTS

To confirm the effectiveness of our proposed DHS for the $(2N+1)$ SHE-PWM problems, we compare it with other algorithms such as DE, HS, GA, PSO, ACO, and TLBO.

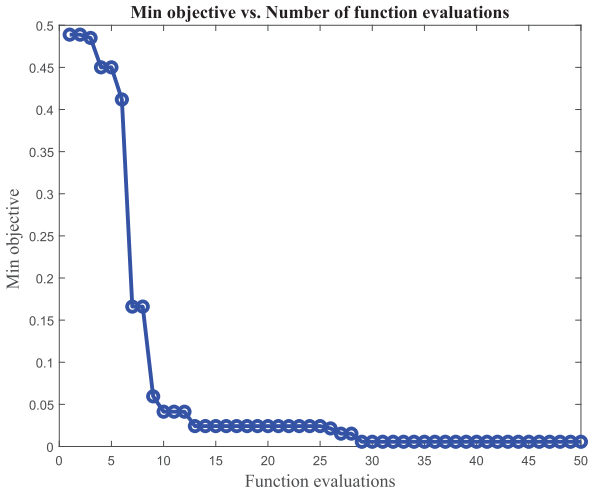

FIGURE 6. Plot of the automatic parameter configuration progress using the Bayesian optimization method.

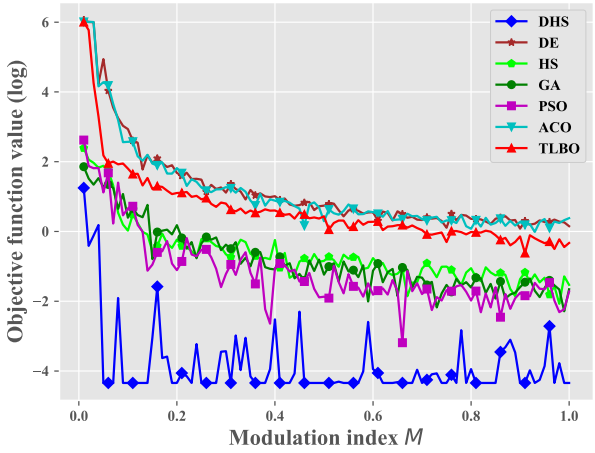

FIGURE 7. The obtained objective function values versus *M*.

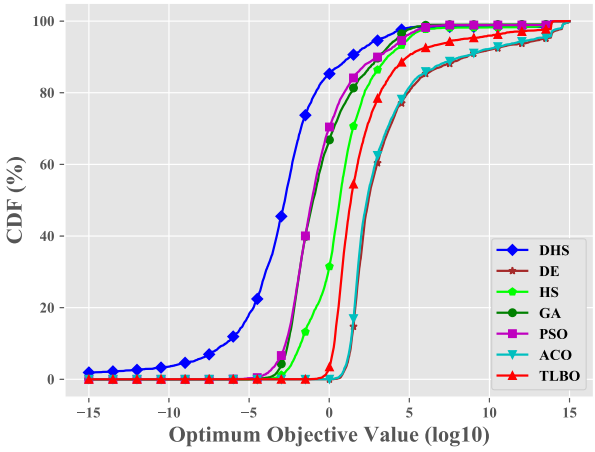

FIGURE 8. Comparison on the CDF curves.

Fig. 7 presents the best solutions obtained by all of the algorithms at different modulation indexes of *M* (The average/standard deviation over 30 trials can be found in Table 4).

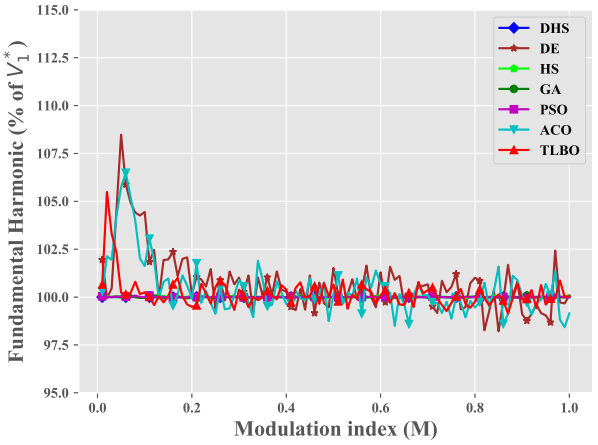

FIGURE 9. The calculated fundamental harmonic compared to V_1^*.

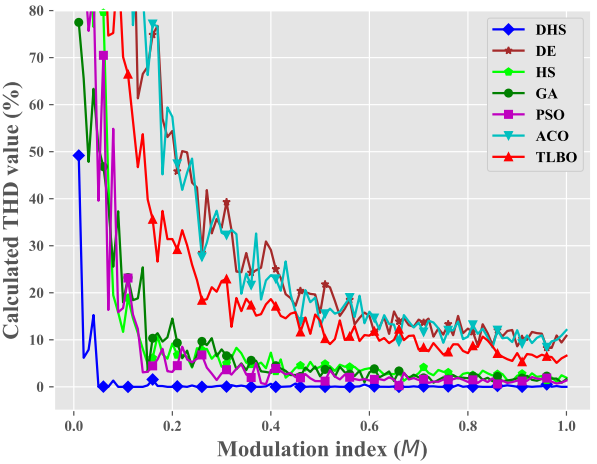

FIGURE 10. The calculated THD versus *M*.

It can be observed that DHS yields the best results on almost all of the 100 problem instances with different modulation indexes, then followed by PSO, GA and HS. TLBO, ACO, and DE show poorer performance than other methods. The advance of DHS compared to the second-best method is also significant since the gap is about two orders of magnitude (i.e., 10^{-4} to 10^{-2}).

Because randomness is the nature of evolutionary/metaheuristic algorithms, an analysis of the robustness of the algorithms is necessary then. Here, the CDF value is applied. The CDF value is an effective metric for estimating the overall performance of an algorithm over a set of problems. It is defined by the probability of a real-valued random variable X that less than or equal to x. In other words, it can be expressed by:

$$CDF(x) = P(X < x), \tag{23}$$

For example, when the results of algorithm $\mathcal{A}$ on $n_p * n_r$ (n_p is number of problems, and n_r is the number of independent trials) problem instances are obtained, and the calculated CDF value at $x = 10^{-5}$ is 40%, it means for 40% of the runs, the obtained results are smaller or equal to 10^{-5}.

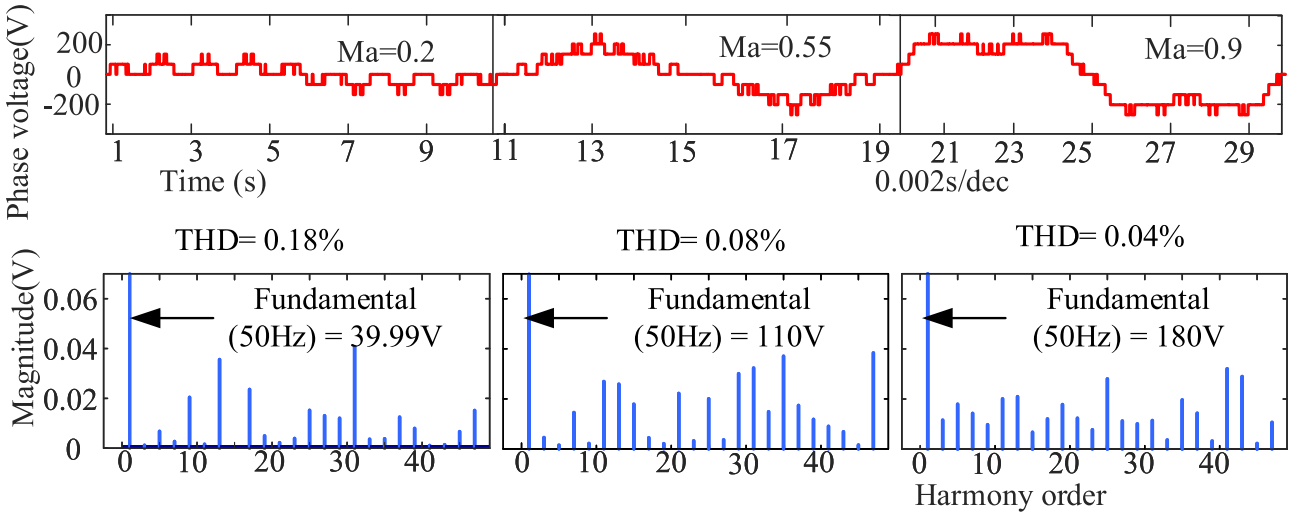

FIGURE 11. Simulation FFT analysis of line voltage by different modulation index.

TABLE 1. Parameter settings of compared algorithms.

Algorithms	Parameters
GA	Population size $PS = 50$, crossover probability $r_c = 0.9$, mutation probability $r_m = 0.1$
PSO	Swarm size $P_n = 50$, $c_1 = c_2 = 2.0$, $\omega_{max} = 0.9$, $\omega_{min} = 0.2$, $V_{max} = (\boldsymbol{UB} - \boldsymbol{LB})$
DE	Population size $PS = 50$, crossover probability $CR = 0.9$, Mutation factor $F = 0.5$
HS	Harmony memory size $HMS = 10$, harmony consideration rate $HMCR = 0.98$, pitch adjustment rate $PAR = 0.9$, bandwidth $BW = 0.1$
ACO	Archive size $n_{Pop} = 50$, sample size $n_{Sample} = 50$, intensification factor $q = 0.5$, deviation-distance ratio $zeta = 1.0$
TLBO [19]	Population size $P = 70$, teaching factor $TF = rand(1, 2)$

TABLE 2. Comparison of average computational times between DHS and other algorithms (Unit: s).

Methods	DHS	DE	HS	GA	PSO	ACO	TLBO
Average	7.02	17.17	43.82	15.50	10.37	16.87	10.47

TABLE 3. Simulation and experiment parameters of MMC.

Parameters	Value
high-voltage level DC source	$400V$
Maximum value of DC source to power control board	120V
Parameters of load	No-load
Number of sub-modules in each arm	4
Highest-order harmonic to be eliminated	49 th
Number of switching angles in first QW	17
Arm resistance R_{arm} and inductor L_{arm}	0.1Ω,4.62mH
Switching Angles	Obtained by DHS
Line frequency	50HZ
Selected orders of harmonics to be eliminated	5th, 7th, 11th, 13th, 17th, 19th, 23rd, 25th, 29th, 31st,35th, 37th, 41st, 43rd,47th, and 49th

Fig. 8 depicts the CDF values of all the methods. It can be observed that about more than 20% of the runs, DHS can yield the objective value smaller than 10^{-5}, 80% of the runs, DHS can yield the objective value smaller than 10^0. For 100% of the runs, DHS can yield the objective value smaller than 10^6, which means DHS can always find feasible solutions. However, some of the methods (i.e, TLBO, ACO, and DE) sometimes failed to find feasible solutions. In addition, the likelihood of converging to global optimum is significantly improved when compared DHS with HS and DE.

Fig. 9 gives the magnitude of fundamental harmonic versus modulation index M. It can be observed that though the desired values at some modulation indexes are not achieved, the results for all methods are still acceptable since the maximum deviation is within 10%.

Fig. 10 presents the calculated THD values for assessing voltage quality. It can be observed that lower THD values are achieved with higher modulation indexes. It's a combined consequence of the increase in the fundamental value and the elimination of the low order harmonics. It also can be found the superiority performance of DHS on the THD values. The obtained THD values can be reduced under 2% for most of the modulation indexes.

Table 2 provides the average computational times for all methods. It can be found that our proposed DHS can finish a single search within 10 seconds, which is shorter than all other methods.

D. SIMULATION RESULTS

A simulation prototype of half-bridge MMC is developed in MATLAB 2018 (b)/Simulink, and its key parameters are depicted in Table 3. According to various modulation indices with a step of 0.01 from 0 to 1, the corresponding switching angles are acquired by proposed DHS and stored in look-up

table, i.e. Table 4 in Appendix B. The modulation indexes are with a high accuracy of 0.01. Its precision is high enough to meet the required sudden changes occurred. For better validating the performance of our proposed DHS, the inverter is with no load in the simulation. Merely under this condition, the output line voltage waveforms can apparently approach the desired values obtained by DHS. Otherwise, if the inverter is with load, the output phase voltage waveform will be caused certain irregular fluctuation by output current. In the simulation test, a 9-level MMC is performed using (2*N*+1) SHE-PWM based on look-up table from Table 4 in Appendix B, in which all the switching angles are obtained by our proposed DHS algorithm.

To test the dynamic changes of modulation index, three groups of switching angles based on three corresponding modulation indices are selected from look-up table in our simulation and its results are depicted in Fig. 11. At the beginning of the simulation, the modulation index is set to 0.2, then the modulation index varies from 0.2 to 0.55 at the end of 1st fundamental period, and further varies from 0.55 to 0.9 at the end of 2nd fundamental period. The line voltage is recorded as shown at the top of Fig. 11, and its THD analysis is depicted at the bottom of Fig. 11. Without considering triple odd harmonics owing to the features of three-phase symmetrical prototype, the THD values are calculated up to 49th harmonic. It can be found that the THD values of various modulation indexes (0.18% for M = 0.2, 0.08% for M = 0.55, 0.04% for M = 0.9) are very low. The magnitudes of selected order harmonics to be eliminated are below 0.07V, and much lower than settled 2% of fundamental component value. In addition, the real phase voltage fundamental amplitude values are almost 39.99V, 110V and 180V. The desired phase voltage fundamental amplitude values are 40V, 110V, and 180V. Thus, the gaps between the real and desired are below 0.01V, only 0.025%, 0% and 0% of corresponding fundamental component amplitudes at modulation indexes of 0.2, 0.55 and 0.9. Therefore, the simulation results demonstrate that our proposed DHS does work very efficiently, and our proposed objective function can provide very tight control of specified low-order harmonics and THD.

V. EXPERIMENTAL RESULTS

In this section, an experimental prototype same as the simulation is developed using various switching angles obtained by DHS. The inverter is no-load as well to better validate the performance of our proposed DHS. The key parameters are the same as the simulation depicted in Table 3 as well.

The experiment platform is shown in Fig. 12. The SMs of the same phase are shown in Fig. 12 (a). The control system is powered by another DC source with maximum output voltage 120V and output current 10A as shown in Fig. 12(b). The detailed structure of MMC chassis is depicted in Fig. 12(c). In Fig. 12 (d), the control system employs a TMS320F2812 DSP from Texas Instruments to store the look-up table, closed-loop circulating current control, capacitors' voltage balancing, and over-current/voltage

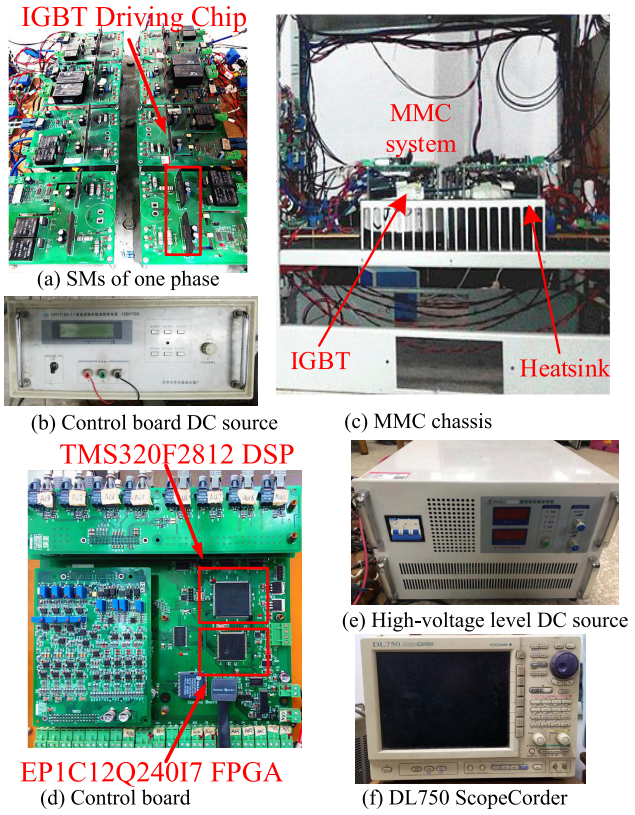

FIGURE 12. Experiment platform.

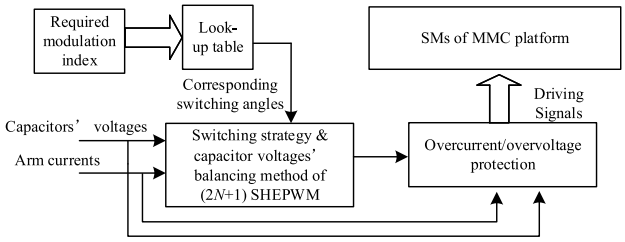

FIGURE 13. Control block diagram for each SM of MMC.

protection with C Language. An EP1C12Q240I7 FPGA from Altera is utilized for pulse-width modulation, gating signal generation, and overvoltage/overcurrent protection with Verilog language. The main circuit of MMC is powered by one high-voltage level DC source as shown in Fig. 12(e). In Fig. 12 (f), A YOKOGAWAD L750 is used to record the line voltage waveform. The whole system operates under fundamental frequency 50Hz, and the sampling frequency is 8 KHz.

The look-up table of switching angles obtained by our proposed DHS algorithm is saved in programmable controller TMS320F2812 DSP as shown in Table 5. As depicted in Fig. 13, at first, according to required modulation index, the corresponding switching angles are acquired by look-up table stored in control system. Then with the captured simultaneous capacitors' voltages, arm currents, and required switching angles, control system employs switching strategy and capacitor voltages' balancing method and

TABLE 4. Comparison of the mean and standard deviation values between DHS, DE, HS, GA, PSO, ACO, and TLBO over 30 independent trials. For each problem instance, the best mean value is in bold.

Modulation index	DHS	DE	HS	GA	PSO	ACO	TLBO
$M = 0.01$	**7.00E+5** (4.66E+5)	2.50E+6 (5.31E+5)	9.75E+5 (1.84E+5)	7.35E+5 (4.47E+5)	8.67E+5 (3.46E+5)	2.52E+6 (5.28E+5)	1.07E+6 (8.14E+4)
$M = 0.02$	**6.33E+5** (4.90E+5)	1.96E+6 (4.37E+5)	5.25E+5 (4.53E+5)	2.01E+5 (4.06E+5)	2.34E+5 (4.30E+5)	1.83E+6 (4.63E+5)	9.97E+5 (7.71E+4)
$M = 0.03$	2.00E+5 (4.07E+5)	1.61E+6 (4.11E+5)	2.41E+4 (9.51E+4)	**1.60E+2** (1.33E+2)	2.39E+2 (1.97E+2)	1.50E+6 (4.31E+5)	4.98E+5 (3.78E+5)
$M = 0.04$	6.67E+4 (2.54E+5)	1.09E+6 (3.74E+5)	9.36E+2 (3.62E+3)	**1.19E+2** (8.98E+1)	1.65E+2 (6.76E+1)	9.14E+5 (3.73E+5)	7.37E+4 (8.88E+4)
$M = 0.05$	**3.98E+1** (3.92E+1)	8.62E+5 (3.01E+5)	2.46E+2 (4.74E+2)	7.07E+1 (3.87E+1)	1.26E+2 (5.90E+1)	7.34E+5 (3.70E+5)	1.97E+4 (2.08E+4)
$M = 0.06$	**2.55E+1** (2.98E+1)	3.81E+5 (2.75E+5)	1.77E+2 (2.20E+2)	6.67E+1 (3.25E+1)	1.38E+2 (1.51E+2)	2.85E+5 (2.43E+5)	5.54E+3 (7.90E+3)
$M = 0.07$	**2.29E+1** (2.09E+1)	2.04E+5 (2.02E+5)	1.22E+2 (1.46E+2)	5.33E+1 (3.47E+1)	6.59E+1 (3.73E+1)	1.04E+5 (9.41E+4)	1.20E+3 (1.32E+3)
$M = 0.08$	**1.77E+1** (2.01E+1)	6.39E+4 (8.05E+4)	7.63E+1 (8.78E+1)	4.23E+1 (2.34E+1)	5.83E+1 (2.67E+1)	4.05E+4 (3.77E+4)	6.43E+2 (6.29E+2)
$M = 0.09$	**1.54E+1** (2.43E+1)	2.17E+4 (1.81E+4)	5.29E+1 (6.67E+1)	3.51E+1 (1.79E+1)	3.56E+1 (1.63E+1)	1.98E+4 (2.47E+4)	2.91E+2 (1.88E+2)
$M = 0.10$	**9.42E+0** (6.91E+0)	1.26E+4 (1.41E+4)	4.81E+1 (4.89E+1)	3.19E+1 (1.38E+1)	3.06E+1 (1.73E+1)	8.70E+3 (1.18E+4)	1.89E+2 (1.05E+2)
$M = 0.11$	**4.38E+0** (4.39E+0)	4.78E+3 (4.34E+3)	4.05E+1 (4.76E+1)	1.79E+1 (7.77E+0)	1.59E+1 (6.89E+0)	6.05E+3 (6.29E+3)	1.42E+2 (8.31E+1)
$M = 0.12$	**4.39E+0** (5.66E+0)	3.37E+3 (2.88E+3)	2.39E+1 (2.99E+1)	2.12E+1 (1.21E+1)	1.51E+1 (1.44E+1)	1.65E+3 (1.71E+3)	1.01E+2 (7.45E+1)
$M = 0.13$	**3.27E+0** (3.63E+0)	2.19E+3 (1.99E+3)	3.01E+1 (4.16E+1)	1.67E+1 (8.74E+0)	8.63E+0 (5.61E+0)	2.23E+3 (2.66E+3)	7.37E+1 (2.94E+1)
$M = 0.14$	**1.47E+0** (2.77E+0)	9.11E+2 (7.99E+2)	2.36E+1 (2.76E+1)	1.23E+1 (4.98E+0)	4.75E+0 (5.27E+0)	7.12E+2 (6.44E+2)	6.73E+1 (2.71E+1)
$M = 0.15$	**1.22E+0** (2.65E+0)	7.91E+2 (1.10E+3)	1.51E+1 (2.12E+1)	8.53E+0 (4.43E+0)	4.42E+0 (4.17E+0)	7.85E+2 (1.07E+3)	5.25E+1 (1.94E+1)
$M = 0.16$	**9.54E-1** (1.88E+0)	4.33E+2 (3.49E+2)	1.48E+1 (2.23E+1)	7.37E+0 (3.59E+0)	2.50E+0 (2.20E+0)	3.41E+2 (2.76E+2)	4.57E+1 (2.10E+1)
$M = 0.17$	**5.06E-1** (5.25E-1)	3.69E+2 (4.15E+2)	1.84E+1 (2.15E+1)	6.59E+0 (3.47E+0)	2.40E+0 (2.25E+0)	2.89E+2 (2.47E+2)	3.76E+1 (1.24E+1)
$M = 0.18$	**7.77E-1** (1.13E+0)	2.22E+2 (1.85E+2)	1.05E+1 (1.82E+1)	4.66E+0 (2.42E+0)	3.49E+0 (2.86E+0)	1.94E+2 (8.70E+1)	3.25E+1 (1.08E+1)
$M = 0.19$	**5.46E-1** (7.23E-1)	2.12E+2 (9.09E+1)	1.46E+1 (1.67E+1)	4.46E+0 (2.72E+0)	3.58E+0 (2.89E+0)	1.52E+2 (7.56E+1)	3.29E+1 (8.48E+0)
$M = 0.20$	**5.86E-1** (1.09E+0)	1.46E+2 (6.86E+1)	1.23E+1 (1.19E+1)	4.69E+0 (1.92E+0)	4.48E+0 (3.94E+0)	1.36E+2 (5.01E+1)	2.55E+1 (7.57E+0)
$M = 0.21$	**8.44E-1** (1.12E+0)	1.49E+2 (7.85E+1)	1.20E+1 (1.34E+1)	4.39E+0 (2.25E+0)	3.81E+0 (2.78E+0)	1.13E+2 (4.48E+1)	2.26E+1 (5.22E+0)
$M = 0.22$	**8.81E-1** (1.13E+0)	1.19E+2 (6.35E+1)	1.08E+1 (1.20E+1)	3.17E+0 (1.78E+0)	4.10E+0 (2.25E+0)	9.71E+1 (4.44E+1)	2.27E+1 (4.38E+0)
$M = 0.23$	**9.27E-1** (1.27E+0)	1.07E+2 (4.17E+1)	9.20E+0 (1.04E+1)	2.92E+0 (1.63E+0)	3.38E+0 (1.98E+0)	8.71E+1 (3.56E+1)	1.76E+1 (4.34E+0)
$M = 0.24$	**4.50E-1** (6.59E-1)	9.34E+1 (3.52E+1)	9.38E+0 (8.39E+0)	2.74E+0 (1.62E+0)	2.42E+0 (1.28E+0)	7.08E+1 (2.57E+1)	1.81E+1 (5.22E+0)
$M = 0.25$	**7.64E-1** (8.41E-1)	7.67E+1 (2.90E+1)	1.14E+1 (9.68E+0)	2.60E+0 (1.45E+0)	2.76E+0 (1.73E+0)	7.10E+1 (3.68E+1)	1.59E+1 (4.57E+0)
$M = 0.26$	**4.02E-1** (4.15E-1)	6.57E+1 (2.74E+1)	9.20E+0 (9.00E+0)	2.54E+0 (1.14E+0)	2.07E+0 (1.08E+0)	6.75E+1 (2.89E+1)	1.47E+1 (3.64E+0)
$M = 0.27$	**3.37E-1** (3.13E-1)	5.65E+1 (1.99E+1)	6.91E+0 (6.84E+0)	2.07E+0 (1.00E+0)	1.45E+0 (9.67E-1)	5.66E+1 (2.63E+1)	1.31E+1 (3.36E+0)
$M = 0.28$	**2.59E-1** (4.23E-1)	5.28E+1 (1.90E+1)	6.39E+0 (5.92E+0)	1.85E+0 (6.83E-1)	1.09E+0 (8.65E-1)	5.31E+1 (2.15E+1)	1.20E+1 (3.36E+0)
$M = 0.29$	**1.28E-1** (2.30E-1)	4.52E+1 (1.53E+1)	7.77E+0 (5.94E+0)	1.67E+0 (8.61E-1)	1.06E+0 (9.92E-1)	4.49E+1 (1.91E+1)	1.11E+1 (2.53E+0)
$M = 0.30$	**1.63E-1** (3.50E-1)	4.51E+1 (1.88E+1)	5.99E+0 (5.37E+0)	1.51E+0 (7.07E-1)	6.85E-1 (5.64E-1)	4.04E+1 (1.40E+1)	1.08E+1 (2.82E+0)
$M = 0.31$	**1.42E-1** (1.90E-1)	4.36E+1 (1.55E+1)	5.00E+0 (5.01E+0)	1.33E+0 (7.28E-1)	6.22E-1 (4.45E-1)	3.88E+1 (1.07E+1)	9.73E+0 (3.46E+0)
$M = 0.32$	**1.86E-1** (2.17E-1)	3.70E+1 (1.12E+1)	5.83E+0 (4.21E+0)	1.21E+0 (4.75E-1)	7.35E-1 (5.07E-1)	3.20E+1 (8.86E+0)	8.61E+0 (2.19E+0)
$M = 0.33$	**1.08E-1** (1.57E-1)	3.61E+1 (1.41E+1)	4.74E+0 (4.31E+0)	1.12E+0 (5.04E-1)	9.79E-1 (6.32E-1)	3.27E+1 (1.02E+1)	7.85E+0 (2.10E+0)
$M = 0.34$	**1.84E-1** (2.01E-1)	3.38E+1 (1.34E+1)	4.33E+0 (3.32E+0)	8.36E-1 (5.75E-1)	9.40E-1 (4.92E-1)	3.01E+1 (1.02E+1)	9.15E+0 (2.15E+0)
$M = 0.35$	**1.92E-1** (2.76E-1)	3.00E+1 (1.12E+1)	5.34E+0 (4.32E+0)	8.72E-1 (5.30E-1)	7.69E-1 (5.32E-1)	2.35E+1 (8.66E+0)	8.50E+0 (2.15E+0)
$M = 0.36$	**2.54E-1** (2.84E-1)	2.63E+1 (9.65E+0)	4.85E+0 (3.38E+0)	9.65E-1 (4.27E-1)	7.57E-1 (5.19E-1)	2.46E+1 (8.93E+0)	7.38E+0 (1.92E+0)
$M = 0.37$	**2.03E-1** (3.04E-1)	2.70E+1 (9.72E+0)	3.85E+0 (3.06E+0)	8.52E-1 (4.53E-1)	9.64E-1 (7.65E-1)	2.36E+1 (7.17E+0)	6.94E+0 (1.78E+0)
$M = 0.38$	**1.58E-1** (2.19E-1)	2.67E+1 (9.93E+0)	4.39E+0 (3.54E+0)	8.39E-1 (3.88E-1)	8.49E-1 (5.12E-1)	1.91E+1 (7.55E+0)	7.11E+0 (1.45E+0)
$M = 0.39$	**1.61E-1** (1.96E-1)	2.09E+1 (7.48E+0)	2.89E+0 (2.84E+0)	7.64E-1 (4.02E-1)	8.85E-1 (5.55E-1)	1.74E+1 (4.49E+0)	6.35E+0 (1.44E+0)
$M = 0.40$	**1.69E-1** (2.30E-1)	2.07E+1 (5.82E+0)	4.49E+0 (2.61E+0)	7.50E-1 (3.69E-1)	8.14E-1 (4.30E-1)	1.83E+1 (6.78E+0)	5.88E+0 (1.08E+0)
$M = 0.41$	**1.95E-1** (2.85E-1)	2.09E+1 (8.59E+0)	3.86E+0 (2.90E+0)	6.62E-1 (2.92E-1)	5.91E-1 (4.10E-1)	1.70E+1 (4.63E+0)	6.06E+0 (1.26E+0)
$M = 0.42$	**1.22E-1** (1.03E-1)	1.87E+1 (5.92E+0)	3.50E+0 (2.58E+0)	6.03E-1 (2.96E-1)	5.95E-1 (3.88E-1)	1.85E+1 (5.14E+0)	5.44E+0 (9.55E-1)
$M = 0.43$	**1.17E-1** (1.10E-1)	1.85E+1 (6.00E+0)	3.77E+0 (3.06E+0)	5.62E-1 (2.73E-1)	4.65E-1 (3.34E-1)	1.57E+1 (5.09E+0)	5.14E+0 (1.33E+0)
$M = 0.44$	**5.49E-2** (7.59E-2)	1.48E+1 (4.69E+0)	2.19E+0 (2.42E+0)	5.43E-1 (2.29E-1)	3.99E-1 (2.44E-1)	1.58E+1 (4.83E+0)	4.84E+0 (1.37E+0)
$M = 0.45$	**1.13E-1** (1.51E-1)	1.45E+1 (5.26E+0)	3.11E+0 (2.31E+0)	5.06E-1 (2.65E-1)	3.38E-1 (2.13E-1)	1.35E+1 (4.36E+0)	4.87E+0 (8.37E-1)
$M = 0.46$	**8.57E-2** (1.02E-1)	1.47E+1 (4.18E+0)	2.48E+0 (1.89E+0)	5.26E-1 (2.06E-1)	4.48E-1 (3.97E-1)	1.16E+1 (4.46E+0)	4.66E+0 (1.04E+0)
$M = 0.47$	**9.33E-2** (1.33E-1)	1.36E+1 (4.57E+0)	2.43E+0 (1.82E+0)	4.47E-1 (1.86E-1)	3.44E-1 (2.31E-1)	1.17E+1 (3.61E+0)	4.33E+0 (1.11E+0)
$M = 0.48$	**9.02E-2** (9.56E-2)	1.24E+1 (4.06E+0)	2.33E+0 (1.97E+0)	4.41E-1 (2.12E-1)	4.54E-1 (3.15E-1)	1.26E+1 (3.53E+0)	4.11E+0 (8.41E-1)
$M = 0.49$	**2.39E-1** (5.28E-1)	1.31E+1 (5.57E+0)	2.59E+0 (1.95E+0)	3.48E-1 (1.57E-1)	3.60E-1 (2.70E-1)	1.12E+1 (4.06E+0)	4.01E+0 (8.75E-1)
$M = 0.50$	**7.41E-2** (9.52E-2)	1.18E+1 (3.92E+0)	2.92E+0 (1.44E+0)	3.54E-1 (2.33E-1)	4.60E-1 (2.77E-1)	1.13E+1 (4.05E+0)	3.99E+0 (7.12E-1)
$M = 0.51$	**1.63E-1** (1.83E-1)	1.16E+1 (3.56E+0)	2.14E+0 (1.62E+0)	3.40E-1 (1.76E-1)	4.35E-1 (3.04E-1)	9.70E+0 (2.80E+0)	3.80E+0 (1.15E+0)
$M = 0.52$	**5.46E-2** (6.59E-2)	1.11E+1 (3.64E+0)	2.52E+0 (1.47E+0)	3.40E-1 (1.59E-1)	5.21E-1 (4.53E-1)	8.97E+0 (3.34E+0)	3.59E+0 (7.60E-1)
$M = 0.53$	**9.55E-2** (1.10E-1)	1.04E+1 (3.71E+0)	2.86E+0 (1.70E+0)	3.65E-1 (1.96E-1)	4.66E-1 (3.05E-1)	9.31E+0 (3.69E+0)	3.62E+0 (6.31E-1)
$M = 0.54$	**1.24E-1** (1.35E-1)	9.91E+0 (3.50E+0)	2.17E+0 (1.74E+0)	3.68E-1 (1.89E-1)	4.02E-1 (2.82E-1)	8.70E+0 (2.60E+0)	3.21E+0 (6.91E-1)
$M = 0.55$	**8.10E-2** (1.10E-1)	9.89E+0 (2.83E+0)	2.35E+0 (1.41E+0)	3.32E-1 (1.66E-1)	3.53E-1 (1.76E-1)	9.26E+0 (2.26E+0)	3.29E+0 (8.41E-1)
$M = 0.56$	**7.11E-2** (8.86E-2)	8.85E+0 (2.56E+0)	2.08E+0 (1.43E+0)	2.98E-1 (1.66E-1)	3.21E-1 (2.36E-1)	7.86E+0 (2.14E+0)	3.00E+0 (7.41E-1)
$M = 0.57$	**7.37E-2** (8.82E-2)	8.65E+0 (2.87E+0)	2.22E+0 (1.25E+0)	2.86E-1 (1.43E-1)	2.93E-1 (2.48E-1)	8.28E+0 (2.48E+0)	3.02E+0 (5.07E-1)
$M = 0.58$	**5.08E-2** (7.92E-2)	8.53E+0 (3.02E+0)	2.03E+0 (1.30E+0)	3.20E-1 (1.65E-1)	2.45E-1 (1.44E-1)	8.04E+0 (2.82E+0)	2.94E+0 (7.84E-1)
$M = 0.59$	**5.55E-2** (7.45E-2)	8.03E+0 (2.42E+0)	1.66E+0 (1.25E+0)	2.51E-1 (1.05E-1)	1.59E-1 (1.28E-1)	7.14E+0 (1.96E+0)	2.77E+0 (5.10E-1)
$M = 0.60$	**5.00E-2** (5.37E-2)	9.15E+0 (2.40E+0)	1.84E+0 (1.09E+0)	2.49E-1 (1.15E-1)	1.81E-1 (1.46E-1)	7.39E+0 (2.14E+0)	3.05E+0 (6.43E-1)
$M = 0.61$	**7.36E-2** (8.27E-2)	7.54E+0 (2.71E+0)	1.81E+0 (1.10E+0)	3.12E-1 (1.59E-1)	1.41E-1 (8.99E-2)	7.21E+0 (2.08E+0)	2.76E+0 (6.28E-1)
$M = 0.62$	**6.51E-2** (9.41E-2)	7.58E+0 (2.33E+0)	1.62E+0 (1.08E+0)	2.57E-1 (1.14E-1)	2.31E-1 (1.56E-1)	6.64E+0 (1.85E+0)	2.43E+0 (6.06E-1)
$M = 0.63$	**7.25E-2** (7.63E-2)	7.70E+0 (2.24E+0)	2.02E+0 (1.17E+0)	2.37E-1 (1.07E-1)	2.97E-1 (1.77E-1)	6.68E+0 (1.74E+0)	2.40E+0 (7.92E-1)
$M = 0.64$	**5.29E-2** (6.56E-2)	6.94E+0 (2.38E+0)	1.26E+0 (1.09E+0)	2.34E-1 (1.03E-1)	2.60E-1 (1.60E-1)	6.61E+0 (2.48E+0)	2.62E+0 (6.25E-1)
$M = 0.65$	**1.38E-1** (2.42E-1)	6.57E+0 (1.67E+0)	1.32E+0 (1.05E+0)	1.88E-1 (1.13E-1)	2.33E-1 (1.62E-1)	6.27E+0 (2.21E+0)	2.57E+0 (7.10E-1)
$M = 0.66$	**8.15E-2** (1.04E-1)	6.69E+0 (2.01E+0)	1.69E+0 (1.20E+0)	2.24E-1 (1.02E-1)	2.19E-1 (1.35E-1)	5.87E+0 (1.99E+0)	2.55E+0 (4.93E-1)
$M = 0.67$	**5.37E-2** (5.90E-2)	6.64E+0 (1.68E+0)	1.36E+0 (9.75E-1)	2.11E-1 (1.17E-1)	2.88E-1 (1.46E-1)	5.76E+0 (1.41E+0)	2.47E+0 (4.03E-1)
$M = 0.68$	**5.40E-2** (7.00E-2)	6.82E+0 (2.03E+0)	1.26E+0 (9.71E-1)	1.44E-1 (9.85E-2)	2.13E-1 (1.19E-1)	5.56E+0 (1.34E+0)	2.47E+0 (4.55E-1)
$M = 0.69$	**4.39E-2** (5.30E-2)	6.24E+0 (1.85E+0)	1.10E+0 (9.36E-1)	1.71E-1 (8.04E-2)	2.25E-1 (1.13E-1)	5.41E+0 (1.68E+0)	2.11E+0 (4.92E-1)
$M = 0.70$	**5.57E-2** (7.05E-2)	5.89E+0 (2.08E+0)	1.24E+0 (9.76E-1)	1.68E-1 (7.78E-2)	2.54E-1 (1.66E-1)	6.15E+0 (2.09E+0)	2.19E+0 (5.80E-1)
$M = 0.71$	**5.76E-2** (4.86E-2)	6.13E+0 (2.03E+0)	1.49E+0 (8.50E-1)	1.47E-1 (6.16E-2)	1.66E-1 (1.02E-1)	5.23E+0 (1.73E+0)	1.99E+0 (6.24E-1)
$M = 0.72$	**4.00E-2** (4.69E-2)	5.89E+0 (2.10E+0)	1.24E+0 (7.91E-1)	1.51E-1 (6.47E-2)	1.62E-1 (8.47E-2)	5.29E+0 (1.59E+0)	2.15E+0 (4.79E-1)
$M = 0.73$	**3.01E-2** (4.71E-2)	5.44E+0 (1.60E+0)	1.41E+0 (9.76E-1)	1.63E-1 (7.00E-2)	1.31E-1 (9.09E-2)	5.32E+0 (1.23E+0)	2.21E+0 (6.15E-1)
$M = 0.74$	**2.68E-2** (3.50E-2)	5.93E+0 (2.84E+0)	1.21E+0 (7.99E-1)	1.30E-1 (7.56E-2)	1.62E-1 (2.53E-1)	5.00E+0 (1.93E+0)	1.94E+0 (5.06E-1)
$M = 0.75$	**3.92E-2** (4.39E-2)	5.32E+0 (1.43E+0)	1.35E+0 (7.88E-1)	1.46E-1 (9.82E-2)	1.35E-1 (1.04E-1)	5.05E+0 (1.11E+0)	2.09E+0 (5.54E-1)
$M = 0.76$	**4.99E-2** (7.63E-2)	5.45E+0 (1.49E+0)	1.31E+0 (6.30E-1)	1.39E-1 (6.57E-2)	1.21E-1 (7.35E-2)	5.05E+0 (1.40E+0)	1.77E+0 (4.12E-1)
$M = 0.77$	**3.38E-2** (4.08E-2)	5.12E+0 (1.73E+0)	9.38E-1 (7.10E-1)	1.35E-1 (5.61E-2)	1.58E-1 (8.12E-2)	5.37E+0 (1.86E+0)	1.86E+0 (4.05E-1)
$M = 0.78$	**6.89E-2** (6.20E-2)	5.36E+0 (1.63E+0)	1.06E+0 (6.80E-1)	1.36E-1 (7.42E-2)	1.76E-1 (7.46E-2)	4.89E+0 (1.56E+0)	1.81E+0 (4.66E-1)
$M = 0.79$	**6.90E-2** (7.02E-2)	5.15E+0 (1.22E+0)	1.01E+0 (7.91E-1)	1.25E-1 (6.32E-2)	1.83E-1 (1.16E-1)	3.92E+0 (1.18E+0)	1.78E+0 (4.62E-1)
$M = 0.80$	**4.85E-2** (4.53E-2)	4.63E+0 (1.36E+0)	1.12E+0 (7.30E-1)	1.51E-1 (1.15E-1)	1.63E-1 (8.21E-2)	4.75E+0 (1.37E+0)	1.76E+0 (4.11E-1)
$M = 0.81$	**3.40E-2** (3.69E-2)	4.63E+0 (1.23E+0)	1.04E+0 (6.99E-1)	1.16E-1 (6.01E-2)	1.92E-1 (1.14E-1)	4.61E+0 (1.54E+0)	1.82E+0 (4.98E-1)
$M = 0.82$	**6.72E-2** (6.57E-2)	5.08E+0 (1.79E+0)	9.15E-1 (6.98E-1)	1.31E-1 (5.77E-2)	1.61E-1 (1.06E-1)	4.90E+0 (1.42E+0)	1.58E+0 (3.88E-1)
$M = 0.83$	**4.27E-2** (6.23E-2)	4.50E+0 (1.84E+0)	1.03E+0 (6.90E-1)	1.18E-1 (5.66E-2)	1.57E-1 (8.55E-2)	4.84E+0 (1.37E+0)	1.76E+0 (4.13E-1)
$M = 0.84$	**3.87E-2** (3.64E-2)	5.05E+0 (2.05E+0)	8.94E-1 (6.45E-1)	1.03E-1 (3.77E-2)	1.40E-1 (8.99E-2)	4.22E+0 (1.25E+0)	1.62E+0 (3.91E-1)
$M = 0.85$	**2.79E-2** (3.29E-2)	4.62E+0 (1.53E+0)	1.00E+0 (6.26E-1)	1.00E-1 (4.36E-2)	1.42E-1 (1.37E-1)	4.15E+0 (1.36E+0)	1.45E+0 (4.66E-1)
$M = 0.86$	**2.64E-2** (2.68E-2)	4.37E+0 (1.21E+0)	7.78E-1 (6.22E-1)	9.68E-2 (3.38E-2)	1.04E-1 (1.03E-1)	5.07E+0 (1.73E+0)	1.48E+0 (4.86E-1)
$M = 0.87$	**2.13E-2** (2.77E-2)	4.75E+0 (1.79E+0)	8.14E-1 (5.90E-1)	8.55E-2 (3.83E-2)	1.15E-1 (9.04E-2)	4.28E+0 (1.24E+0)	1.38E+0 (3.62E-1)
$M = 0.88$	**2.35E-2** (2.17E-2)	4.62E+0 (1.60E+0)	5.75E-1 (5.55E-1)	7.45E-2 (3.25E-2)	6.77E-2 (4.93E-2)	4.34E+0 (1.33E+0)	1.38E+0 (4.57E-1)
$M = 0.89$	**3.55E-2** (3.32E-2)	4.49E+0 (1.30E+0)	8.22E-1 (6.52E-1)	9.60E-2 (4.39E-2)	1.03E-1 (7.57E-2)	4.39E+0 (1.47E+0)	1.51E+0 (4.00E-1)
$M = 0.90$	**4.10E-2** (4.01E-2)	4.62E+0 (1.73E+0)	7.32E-1 (5.33E-1)	9.10E-2 (3.58E-2)	1.08E-1 (1.14E-1)	4.39E+0 (1.57E+0)	1.39E+0 (2.90E-1)
$M = 0.91$	**6.25E-2** (5.74E-2)	4.71E+0 (1.48E+0)	6.69E-1 (5.30E-1)	9.25E-2 (4.52E-2)	1.32E-1 (1.04E-1)	4.72E+0 (1.81E+0)	1.38E+0 (4.92E-1)
$M = 0.92$	**3.23E-2** (3.26E-2)	4.38E+0 (1.86E+0)	6.01E-1 (5.34E-1)	1.04E-1 (4.26E-2)	1.05E-1 (6.58E-2)	4.18E+0 (1.58E+0)	1.55E+0 (4.51E-1)
$M = 0.93$	**2.59E-2** (3.27E-2)	3.85E+0 (1.41E+0)	6.11E-1 (5.71E-1)	1.10E-1 (5.22E-2)	1.12E-1 (5.22E-2)	4.09E+0 (1.51E+0)	1.39E+0 (4.75E-1)
$M = 0.94$	**3.91E-2** (3.87E-2)	4.72E+0 (1.64E+0)	5.65E-1 (4.35E-1)	9.24E-2 (4.53E-2)	1.25E-1 (7.12E-2)	4.40E+0 (1.50E+0)	1.31E+0 (3.84E-1)
$M = 0.95$	**4.55E-2** (5.47E-2)	4.55E+0 (1.56E+0)	6.38E-1 (5.78E-1)	1.01E-1 (4.62E-2)	1.40E-1 (9.21E-2)	4.80E+0 (1.99E+0)	1.32E+0 (4.03E-1)
$M = 0.96$	**3.80E-2** (4.06E-2)	4.70E+0 (1.95E+0)	6.12E-1 (5.87E-1)	8.25E-2 (3.19E-2)	1.38E-1 (7.72E-2)	4.50E+0 (1.86E+0)	1.37E+0 (4.54E-1)
$M = 0.97$	**3.60E-2** (3.08E-2)	5.21E+0 (2.02E+0)	5.24E-1 (5.01E-1)	9.75E-2 (6.47E-2)	1.16E-1 (6.10E-2)	4.52E+0 (1.72E+0)	1.45E+0 (5.40E-1)
$M = 0.98$	**3.98E-2** (4.31E-2)	4.73E+0 (2.09E+0)	4.35E-1 (4.97E-1)	8.34E-2 (3.56E-2)	1.06E-1 (6.07E-2)	4.76E+0 (2.88E+0)	1.48E+0 (3.87E-1)
$M = 0.99$	**3.21E-2** (3.35E-2)	4.77E+0 (2.19E+0)	5.76E-1 (6.05E-1)	8.22E-2 (5.01E-2)	8.23E-2 (4.28E-2)	4.50E+0 (2.27E+0)	1.15E+0 (4.46E-1)
$M = 1.00$	**2.51E-2** (2.72E-2)	4.82E+0 (1.99E+0)	3.94E-1 (4.58E-1)	6.67E-2 (2.96E-2)	8.60E-2 (6.07E-2)	4.73E+0 (1.69E+0)	1.32E+0 (4.27E-1)

TABLE 5. The switching angles obtained by DHS at different modulation indexes.

Modulation index	θ_1	θ_2	θ_3	θ_4	θ_5	θ_6	θ_7	θ_8	θ_9	θ_{10}	θ_{11}	θ_{12}	θ_{13}	θ_{14}	θ_{15}	θ_{16}	θ_{17}
$M = 0.01$	0.0000	0.0064	0.0107	0.0146	0.1390	0.1447	0.2504	0.2564	0.7556	0.7630	0.8614	0.8695	0.9685	0.9768	1.4467	1.4539	1.5672
$M = 0.02$	0.0571	0.0659	0.2868	0.2984	0.6995	0.7014	0.7525	0.7673	0.8745	0.8801	0.9814	0.9975	1.2180	1.2282	1.4493	1.4628	1.5639
$M = 0.03$	0.0000	0.0090	0.0556	0.0677	0.1673	0.1827	0.7526	0.7588	0.8604	0.8843	0.9768	1.0010	1.3295	1.3467	1.4440	1.4648	1.5603
$M = 0.04$	0.0000	0.0358	0.1486	0.1699	0.2679	0.2920	0.3861	0.4124	0.6221	0.6517	0.7390	0.7703	0.8559	0.8879	0.9732	1.0056	1.5567
$M = 0.05$	0.0511	0.0728	0.1636	0.1893	0.2772	0.3064	0.3915	0.4237	0.6213	0.6583	0.7368	0.7754	0.8527	0.8924	0.9688	1.0091	1.5534
$M = 0.06$	0.0493	0.0752	0.2742	0.3092	0.3881	0.4268	0.6178	0.6624	0.7337	0.7806	0.8683	0.8838	0.9638	1.0128	1.2082	1.2390	1.5499
$M = 0.07$	0.0502	0.0803	0.1604	0.1961	0.2724	0.3130	0.3855	0.4304	0.6137	0.6655	0.7288	0.7829	0.8445	0.9002	0.9607	1.0171	1.5465
$M = 0.08$	0.1563	0.1971	0.2682	0.3147	0.3812	0.4327	0.6101	0.6694	0.7255	0.7879	0.8423	0.9077	0.9846	1.0123	1.0924	1.1268	1.5429
$M = 0.09$	0.0503	0.0886	0.1582	0.2036	0.2683	0.3200	0.3798	0.4372	0.6061	0.6725	0.7207	0.7903	0.8362	0.9079	0.9524	1.0252	1.5396
$M = 0.10$	0.0505	0.0930	0.1574	0.2076	0.2665	0.3237	0.3771	0.4407	0.6022	0.6759	0.7165	0.7938	0.8319	0.9116	0.9482	1.0292	1.5363
$M = 0.11$	0.0509	0.0976	0.1569	0.2119	0.2649	0.3276	0.3746	0.4442	0.5983	0.6792	0.7122	0.7972	0.8275	0.9153	0.9439	1.0332	1.5329
$M = 0.12$	0.1554	0.2154	0.2629	0.3310	0.3718	0.4475	0.5946	0.6830	0.7086	0.8021	0.8248	0.9239	0.9927	1.0348	1.0967	1.1480	1.5296
$M = 0.13$	0.1529	0.2173	0.2592	0.3325	0.6099	0.6172	0.6991	0.8028	0.8179	0.9290	0.9935	1.0386	1.0958	1.1507	1.4145	1.4963	1.5248
$M = 0.14$	0.0521	0.1126	0.1572	0.2271	0.2630	0.3415	0.3695	0.4559	0.5854	0.6853	0.6956	0.8017	0.8085	0.9214	0.9259	1.0453	1.5241
$M = 0.15$	0.2144	0.2973	0.3233	0.4146	0.4323	0.5179	0.5415	0.6502	0.6551	0.8708	0.9401	0.9901	1.0470	1.1084	1.1542	1.2262	1.5643
$M = 0.16$	0.1054	0.1695	0.2095	0.2966	0.3163	0.4062	0.4182	0.4869	0.5596	0.7591	0.7672	0.9945	1.0466	1.1117	1.2128	1.2235	1.5362
$M = 0.17$	0.0521	0.1287	0.1610	0.2268	0.3634	0.4526	0.5871	0.7052	0.7852	0.9262	0.9450	1.0572	1.2544	1.2664	1.3024	1.4007	1.5010
$M = 0.18$	0.0280	0.0721	0.0988	0.1760	0.2193	0.2917	0.6244	0.6390	0.7264	0.9328	0.9575	1.0598	1.2412	1.2643	1.3483	1.5467	1.5514
$M = 0.19$	0.0522	0.1394	0.1603	0.2806	0.2939	0.3531	0.3744	0.4668	0.5727	0.7994	0.8320	0.9136	0.9493	1.0655	1.3808	1.4084	1.5008
$M = 0.20$	0.0512	0.1412	0.1568	0.3032	0.3155	0.3435	0.6031	0.6134	0.6865	0.7976	0.8375	0.9106	0.9539	1.0694	1.3735	1.5081	1.5267
$M = 0.21$	0.0583	0.1013	0.1640	0.2234	0.2680	0.3446	0.4506	0.4760	0.5635	0.5985	0.6759	1.0738	1.1379	1.1899	1.2563	1.3048	1.3758
$M = 0.22$	0.1805	0.1896	0.2074	0.4792	0.5579	0.6719	0.6997	0.7765	0.8307	0.9381	0.9788	1.0617	1.0853	1.2085	1.3851	1.4046	1.4951
$M = 0.23$	0.0623	0.0986	0.1667	0.2198	0.3339	0.3598	0.4447	0.4829	0.5552	0.6041	0.6669	0.7246	0.7802	1.0822	1.1305	1.1990	1.2498
$M = 0.24$	0.0676	0.1022	0.1837	0.1837	0.2177	0.3471	0.3776	0.4850	0.5498	0.7741	0.8471	1.0865	1.1270	1.2042	1.3683	1.4334	1.4890
$M = 0.25$	0.0422	0.1768	0.2336	0.2918	0.3303	0.4076	0.6202	0.9100	0.9834	1.0838	1.2139	1.2856	1.3188	1.3845	1.4209	1.5094	1.5505
$M = 0.26$	0.0733	0.2140	0.2400	0.3522	0.3832	0.4909	0.5409	0.7628	0.8508	0.8778	0.9476	1.0941	1.1165	1.1441	1.3644	1.4442	1.4848
$M = 0.27$	0.0805	0.1052	0.1822	0.3505	0.3833	0.4929	0.5360	0.7648	0.8194	1.1019	1.1186	1.2284	1.2544	1.2857	1.3579	1.4486	1.4825
$M = 0.28$	0.0553	0.1379	0.1586	0.2328	0.2700	0.3309	0.3839	0.4991	0.5349	0.6411	0.7335	0.7508	0.8543	0.8656	0.9795	1.1068	1.4789
$M = 0.29$	0.0943	0.1900	0.2256	0.2869	0.3381	0.5945	0.6077	0.6769	0.7707	0.7773	0.8727	0.8747	0.9347	1.1601	1.4319	1.4972	1.5309
$M = 0.30$	0.0000	0.0321	0.1368	0.2904	0.4419	0.5231	0.5433	0.6303	0.7094	0.8083	0.8820	0.9877	0.9960	1.2179	1.2859	1.3873	1.4554
$M = 0.31$	0.0450	0.1456	0.1702	0.2408	0.2880	0.3354	0.4056	0.6179	0.9996	1.1108	1.2071	1.2201	1.3191	1.3262	1.4786	1.5394	1.5478
$M = 0.32$	0.0686	0.0962	0.2899	0.3458	0.4691	0.5903	0.6657	0.8171	0.8513	0.9794	1.0034	1.2097	1.2503	1.2864	1.3137	1.4211	1.5003
$M = 0.33$	0.0451	0.1499	0.1719	0.1807	0.2407	0.2831	0.3328	0.4207	0.4359	0.6472	0.6594	0.8629	1.0066	1.1199	1.2028	1.3190	1.3409
$M = 0.34$	0.0523	0.0728	0.2862	0.3671	0.3842	0.5843	0.5970	0.6897	0.7131	0.8251	0.8532	0.9945	1.0230	1.1606	1.1945	1.2401	1.3000
$M = 0.35$	0.0360	0.1734	0.1907	0.2992	0.3467	0.4109	0.4349	0.7883	1.0212	1.1120	1.1678	1.2070	1.2696	1.3773	1.4071	1.4898	1.5096
$M = 0.36$	0.0450	0.1621	0.1727	0.2442	0.2786	0.3315	0.3888	0.5235	0.5431	0.6300	1.0179	1.1331	1.1935	1.2460	1.3117	1.3564	1.4308
$M = 0.37$	0.0483	0.0933	0.2185	0.2452	0.3085	0.3612	0.3988	0.5252	0.5522	0.9581	1.0221	1.1882	1.2481	1.3053	1.3572	1.4231	1.4638
$M = 0.38$	0.0461	0.0953	0.3121	0.3634	0.4009	0.5189	0.5523	0.7981	0.8234	0.9525	1.0257	1.1871	1.2618	1.2848	1.3620	1.4218	1.4699
$M = 0.39$	0.0412	0.1274	0.1969	0.4128	0.6089	0.6938	0.7430	0.7775	0.8625	0.9270	1.0315	1.1356	1.2638	1.4451	1.5118	1.5209	1.5572
$M = 0.40$	0.0395	0.1447	0.1701	0.2966	0.3442	0.4665	0.4816	0.6576	0.8418	0.8739	1.0401	1.1133	1.1368	1.3305	1.3706	1.4891	1.5416
$M = 0.41$	0.0450	0.1071	0.1377	0.2417	0.3111	0.3579	0.3997	0.5070	0.5590	0.8240	0.9167	0.9380	1.0376	1.2980	1.3796	1.4169	1.4848
$M = 0.42$	0.1145	0.2588	0.6119	0.6423	0.7002	0.7605	0.9380	0.9813	1.0112	1.0679	1.1287	1.2798	1.3035	1.3367	1.4366	1.4748	1.5405
$M = 0.43$	0.0389	0.0954	0.1123	0.2991	0.3180	0.3933	0.4207	0.4990	0.5583	0.6947	0.7871	0.8002	1.0456	1.1805	1.1865	1.4231	1.5002
$M = 0.44$	0.0347	0.1090	0.2986	0.4107	0.4395	0.6916	0.7753	0.9604	1.0493	1.1371	1.3245	1.3665	1.3679	1.4130	1.4724	1.4914	1.5537
$M = 0.45$	0.0379	0.0943	0.2773	0.3017	0.3591	0.4412	0.6339	0.9027	0.9059	0.9268	1.0534	1.1550	1.2535	1.2583	1.4464	1.5321	1.5513
$M = 0.46$	0.0905	0.1627	0.2720	0.2958	0.3584	0.4528	0.5248	0.5471	0.6285	0.8758	0.9961	1.0449	1.1163	1.2035	1.3080	1.3151	1.4588
$M = 0.47$	0.0766	0.2044	0.2178	0.3151	0.3534	0.4863	0.5764	0.6472	0.8747	0.8982	1.0150	1.0519	1.1108	1.3095	1.3246	1.4426	1.5064
$M = 0.48$	0.0466	0.1029	0.1337	0.3008	0.3496	0.3881	0.4433	0.5849	0.7074	0.7230	1.0654	1.1418	1.1757	1.2562	1.2832	1.5074	1.5655
$M = 0.49$	0.0491	0.3073	0.3696	0.4048	0.5057	0.5235	0.5548	0.5669	0.6921	0.7148	0.9095	0.9432	1.0696	1.1349	1.1446	1.2593	1.2940
$M = 0.50$	0.3021	0.3244	0.3737	0.4212	0.4477	0.8912	0.9166	0.9705	1.0248	1.0528	1.2259	1.2536	1.3173	1.3518	1.4330	1.4545	1.5685
$M = 0.51$	0.1105	0.2353	0.4025	0.6083	0.6944	0.7841	0.8219	0.8528	0.9891	1.0262	1.1453	1.1792	1.2093	1.3340	1.3743	1.4656	1.5684
$M = 0.52$	0.0531	0.0973	0.1383	0.2093	0.3140	0.3421	0.3944	0.4524	0.5762	0.8449	1.0824	1.1298	1.1969	1.3075	1.3702	1.4142	1.4921
$M = 0.53$	0.0642	0.0777	0.1664	0.4959	0.5685	0.6391	0.6876	0.7197	0.9113	0.9519	1.0453	1.0641	1.2534	1.3021	1.3688	1.3915	1.5479
$M = 0.54$	0.0427	0.1245	0.2108	0.2697	0.4219	0.4770	0.5594	0.6621	0.6980	0.7885	0.8581	0.9741	1.0898	1.2013	1.3471	1.4596	1.5048
$M = 0.55$	0.2895	0.4159	0.5999	0.6770	0.7431	0.8285	0.8463	0.9112	0.9616	0.9931	1.1614	1.1926	1.2479	1.3094	1.4649	1.5146	1.5372
$M = 0.56$	0.0424	0.1230	0.1781	0.2032	0.2844	0.4314	0.4458	0.5927	0.6445	0.6849	0.7541	0.9820	1.0978	1.2084	1.2278	1.3119	1.5546
$M = 0.57$	0.2791	0.4791	0.5446	0.6439	0.7107	0.7444	0.7874	0.8832	0.9320	0.9689	1.1407	1.1753	1.2292	1.3014	1.3719	1.3803	1.4944
$M = 0.58$	0.0000	0.1152	0.1617	0.3780	0.3936	0.4622	0.6008	0.6316	0.6904	0.7072	0.8522	1.0158	1.0794	1.2473	1.3176	1.3275	1.5463
$M = 0.59$	0.0000	0.0379	0.1167	0.3793	0.4686	0.5151	0.5579	0.6206	0.7143	0.7245	0.8472	0.8832	0.9905	0.9989	1.2174	1.2520	1.4495
$M = 0.60$	0.0340	0.1224	0.1667	0.3580	0.3906	0.4255	0.4555	0.5810	0.8445	1.0035	1.1063	1.1881	1.1965	1.2459	1.4218	1.4363	1.5437
$M = 0.61$	0.0700	0.2494	0.3188	0.3380	0.4516	0.5745	0.6474	0.8174	0.8820	0.9460	1.0037	1.0199	1.1614	1.2029	1.2869	1.4555	1.5414
$M = 0.62$	0.0379	0.1221	0.1976	0.2160	0.3701	0.4073	0.4459	0.6959	0.6982	0.8665	0.8928	1.0074	1.1193	1.3200	1.3349	1.5215	1.5410
$M = 0.63$	0.0381	0.1223	0.2107	0.2255	0.3685	0.4063	0.4803	0.5671	0.6014	0.8606	0.8947	1.0109	1.1241	1.3188	1.3405	1.4763	1.5006
$M = 0.64$	0.0542	0.1060	0.1781	0.3032	0.3295	0.4058	0.4891	0.5796	0.7675	0.7969	0.9712	1.0168	1.1865	1.2266	1.4108	1.4250	1.5097
$M = 0.65$	0.0450	0.0940	0.1254	0.2874	0.3157	0.4079	0.4303	0.4752	0.4895	0.6620	0.7578	0.7937	0.8593	0.9073	0.9650	1.0196	1.4131
$M = 0.66$	0.0349	0.1397	0.1740	0.2214	0.2572	0.2961	0.3637	0.4002	0.4451	0.7402	0.7835	1.0222	1.1376	1.1908	1.2484	1.4316	1.4554
$M = 0.67$	0.0364	0.1197	0.1798	0.2149	0.2402	0.4126	0.5970	0.6698	0.9133	1.0270	1.1381	1.2435	1.2930	1.3404	1.3958	1.4822	1.5703
$M = 0.68$	0.0357	0.1429	0.1677	0.2712	0.3192	0.3756	0.4093	0.4490	0.7281	0.7861	0.8344	1.0299	1.1478	1.1860	1.4311	1.4684	1.5638
$M = 0.69$	0.0245	0.0788	0.2339	0.2669	0.3941	0.4243	0.4551	0.5762	0.6742	0.7760	0.8489	0.8827	0.9680	1.0443	1.1009	1.3660	1.4864
$M = 0.70$	0.0247	0.3088	0.3900	0.4264	0.4581	0.7362	0.7991	0.8353	0.8736	1.0505	1.0919	1.1149	1.2718	1.3070	1.4233	1.4838	1.5225
$M = 0.71$	0.0332	0.1755	0.2099	0.2469	0.3222	0.4206	0.4553	0.6608	0.7259	1.0447	1.1249	1.1355	1.2318	1.2511	1.3353	1.4857	1.5284
$M = 0.72$	0.0379	0.2242	0.2747	0.3854	0.4106	0.5149	0.5494	0.6051	0.7683	0.7864	0.8617	1.0461	1.1661	1.1699	1.2393	1.3982	1.4328
$M = 0.73$	0.0387	0.1182	0.2325	0.3426	0.4796	0.5424	0.6302	0.6946	0.7809	0.8559	0.9300	1.0503	1.1678	1.2425	1.3213	1.3794	1.5050
$M = 0.74$	0.0393	0.0731	0.2663	0.3598	0.4224	0.5135	0.5613	0.6763	0.8141	0.8524	0.9702	1.0508	1.1137	1.2318	1.2713	1.3968	1.4907
$M = 0.75$	0.0563	0.3930	0.4227	0.4985	0.5518	0.5925	0.7819	0.8144	0.8489	1.0292	1.0661	1.1049	1.2187	1.2576	1.3007	1.4009	1.4180
$M = 0.76$	0.0000	0.0356	0.0597	0.1157	0.1920	0.2235	0.2630	0.4010	0.4650	0.6108	0.9256	1.0617	1.1434	1.2565	1.2715	1.4628	1.5505
$M = 0.77$	0.0350	0.0919	0.2168	0.2473	0.4283	0.5868	0.6500	0.7649	0.7769	0.8527	0.9713	1.0622	1.1518	1.2187	1.4490	1.5238	1.5608
$M = 0.78$	0.0000	0.1904	0.2262	0.2871	0.3900	0.5919	0.6302	0.7826	0.8627	0.9679	1.0070	1.0518	1.1951	1.3333	1.4681	1.5173	1.5620
$M = 0.79$	0.0475	0.1194	0.1809	0.2653	0.4825	0.5891	0.6347	0.8352	0.9065	1.0747	1.1374	1.2972	1.3943	1.4180	1.4838	1.5297	1.5498
$M = 0.80$	0.0854	0.2209	0.4004	0.4289	0.4605	0.7630	0.7924	0.9992	1.0312	1.1407	1.1871	1.2291	1.2591	1.2689	1.3964	1.4134	1.5629
$M = 0.81$	0.0381	0.1015	0.2528	0.3332	0.4744	0.4978	0.6261	0.7080	0.7594	0.8272	0.9723	1.0799	1.1815	1.2251	1.3068	1.4084	1.4624
$M = 0.82$	0.0448	0.0667	0.2355	0.2811	0.3638	0.4285	0.4572	0.4731	0.6692	0.7391	0.9510	1.0442	1.0628	1.1850	1.2531	1.3059	1.4515
$M = 0.83$	0.0405	0.1090	0.2121	0.2277	0.3362	0.5888	0.6287	0.6558	0.7226	0.7803	0.9711	1.0920	1.2066	1.2463	1.4275	1.4693	1.5656
$M = 0.84$	0.0927	0.1382	0.1787	0.2068	0.3199	0.4776	0.5948	0.6328	0.7338	0.7787	0.8830	0.9743	0.9975	1.2428	1.4083	1.4490	1.5170
$M = 0.85$	0.0642	0.1157	0.1517	0.2897	0.3135	0.3544	0.4076	0.4567	0.6741	0.7311	0.7708	0.8509	0.8751	1.1032	1.1187	1.4808	1.5118
$M = 0.86$	0.0406	0.0706	0.1077	0.2883	0.4189	0.5673	0.5909	0.7964	0.8182	0.9151	1.0037	1.0868	1.1893	1.3681	1.4048	1.4535	1.5674
$M = 0.87$	0.0629	0.0954	0.1296	0.3555	0.4070	0.4712	0.4903	0.5189	0.6790	0.7241	0.7860	0.8662	0.8715	1.3238	1.3610	1.4546	1.5016
$M = 0.88$	0.0579	0.1228	0.2628	0.2978	0.3390	0.4055	0.5012	0.5242	0.5843	0.6702	0.7413	0.7583	0.9626	1.0379	1.0423	1.1374	1.4604
$M = 0.89$	0.0532	0.0946	0.1296	0.2659	0.3110	0.3447	0.5094	0.5451	0.5976	0.6609	0.6876	0.7849	0.7905	0.9833	1.0006	1.2085	1.2179
$M = 0.90$	0.0000	0.0478	0.0974	0.3272	0.4879	0.5199	0.5709	0.6301	0.6556	0.7470	0.7890	0.8920	0.9080	0.9861	1.0087	1.2967	1.3382
$M = 0.90$	0.0815	0.1085	0.1372	0.2625	0.3446	0.5930	0.6537	0.6804	0.7349	1.0897	1.1146	1.2034	1.2199	1.3607	1.4509	1.4580	1.5504
$M = 0.91$	0.0301	0.1043	0.1493	0.2422	0.3170	0.4696	0.6041	0.6295	0.7352	0.7493	0.7823	0.8797	1.0107	1.1145	1.1909	1.3308	1.5465
$M = 0.92$	0.0725	0.0727	0.0961	0.1549	0.2714	0.3046	0.4560	0.4883	0.5365	0.5981	0.6196	0.7969	0.9181	1.0774	1.1126	1.2062	1.2788
$M = 0.93$	0.0777	0.2173	0.2556	0.4334	0.4608	0.4857	0.5259	0.5847	0.7439	0.8245	0.8531	0.9158	0.9548	1.0604	1.0888	1.3375	1.4920
$M = 0.94$	0.1148	0.2384	0.3095	0.4172	0.4368	0.5816	0.7827	0.8564	0.8799	1.0754	1.1324	1.1937	1.2168	1.3403	1.4570	1.4633	1.5381
$M = 0.95$	0.0398	0.1049	0.1509	0.2802	0.4010	0.4225	0.4632	0.7027	0.7220	0.9691	1.0261	1.1702	1.2196	1.2716	1.3083	1.5388	1.5536
$M = 0.96$	0.0000	0.1869	0.2571	0.2830	0.3998	0.5883	0.6330	0.7283	0.8794	0.9225	1.0412	1.0876	1.1152	1.2684	1.3275	1.4821	1.5283
$M = 0.97$	0.0430	0.1696	0.1833	0.2924	0.3534	0.4271	0.5188	0.5671	0.6818	0.8783	0.9473	0.9770	1.0367	1.2597	1.3162	1.3788	1.5357
$M = 0.98$	0.0000	0.0802	0.1030	0.1745	0.2256	0.3213	0.3822	0.5916	0.6538	0.7823	0.8288	0.9396	1.0341	1.1861	1.3676	1.4724	1.5131
$M = 0.99$	0.0244	0.1356	0.1929	0.2433	0.2849	0.3100	0.3208	0.3703	0.4559	0.6627	0.7233	0.8232	1.0381	1.1615	1.1852	1.3097	1.4645
$M = 1.00$	0.0248	0.1396	0.1961	0.2367	0.3730	0.4566	0.6603	0.7149	0.7674	0.8139	1.0421	1.1718	1.1880	1.3117	1.3263	1.4721	1.5678

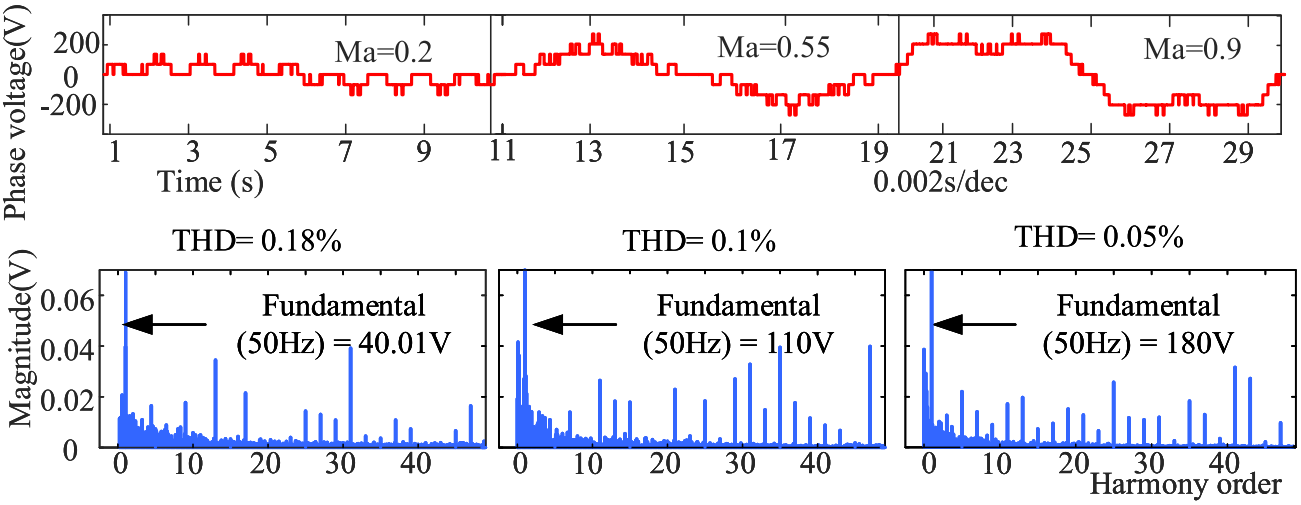

FIGURE 14. Experiment FFT analysis of line voltage by different modulation index.

overcurrent/overvoltage protection to generate driving signals of SMs of MMC.

At the beginning of the experiment, the modulation index is set to 0.2, then varies from 0.2 to 0.55, and then from 0.55 to 0.9 same as the simulation. The value of line voltage is recorded by DL750 ScopeCorder, and the corresponding phase voltage is shown on the top of Fig. 14. Its THD analysis is depicted in the bottom of Fig. 14. The THD values are calculated up to 49th harmonic due to practical operation without considering triplen odd harmonics. It can be observed that the THD values of various modulation indexes (0.18% for M = 0.2, 0.1% for M = 0.55, 0.05% for M = 0.9) are very low. The corresponding phase voltage fundamental amplitude values are almost 40.01V, 110V and 180V. The desired phase voltage fundamental amplitude values are 40V, 110V, and 180V. Thus, the gaps between the real and desired fundamental component amplitudes are very small, only 0.025%, 0% and 0% of corresponding fundamental component amplitudes at modulation indexes of 0.2, 0.55 and 0.9, much lower than settled upper bound 10%. In addition, the magnitudes of target eliminated order harmonics are all lower than 0.7V during the variations of M = 0.2, M = 0.55, and M = 0.9, and are maintained below settled 2% of fundamental component value. Both of them are much lower than the upper bound (10%). Therefore, the success of the experiment confirms the capability of our proposed DHS for practical use.

VI. CONCLUSION

In this paper, a differential harmony search algorithm (DHS) is proposed to solve the (2N+1) SHE-PWM problem. The performance of DHS is compared with 6 other metaheuristic algorithms including DE, HS, GA, PSO, ACO, and TLBO. The comparison has been conducted by running these algorithms on a set of 100 different (2N+1) SHE-PWM problems with modulation indexes vary from 0.01 to 1.0 with a step of 0.01. Based on the comparison of final objective function values, algorithm robustness, the magnitude of fundamental harmonic, and the calculated THD values, it can conclude that DHS has superior performance than the other 6 algorithms for solving the (2N+1) SHE-PWM problem. The switching angles obtained by DHS have been further validated with both simulation and hardware experiments.

Appendix A
FORMULATION OF THE PARAMETER CONFIGURATION

Assume we want to search for optimal parameters in algorithm A on a set of minimization problem instances, let $\boldsymbol{\phi} = (\phi_1, \phi_2, \cdots, \phi_r)$ be the parameter vector, and r is the number of the parameters need to be tuned. During the parameter tuning process, algorithm A will run on n_p problem instances and each instance is repeated for n_t times. For the jth run on the ith instance, the final objective function value obtained by algorithm A with parameter configuration $\boldsymbol{\phi}$ is denoted as $F_{i,j}(\boldsymbol{\phi})$. The best and worst objective function value found so far on the ith instance are denoted as F^i_{min} and F^i_{max}, respectively. Therefore, the objective function for the parameter configuration problem can be formulated as:

$$F_H(\boldsymbol{\phi}) = \frac{\sum_{i=1}^{n_p} \sum_{j=1}^{n_t} \frac{F_{i,j}(\boldsymbol{\phi}) - F^i_{min}}{F^i_{max} - F^i_{min}}}{n_p \cdot n_t}, \tag{24}$$

Please note that the best and worst objective function value on instance i may be changed during the optimization process, thus the objective function for the parameter configuration problem needs to be re-calculated at the end of each iteration.

Appendix B

See tables 4 and 5.

REFERENCES

[1] A. Lesnicar and R. Marquardt, "An innovative modular multilevel converter topology suitable for a wide power range," in *Proc. IEEE Bologna Power Tech Conf.*, vol. 3, Jun. 2003, pp. 1–6.

[2] M. A. Perez, S. Bernet, J. Rodriguez, S. Kouro, and R. Lizana, "Circuit topologies, modeling, control schemes, and applications of modular multilevel converters," *IEEE Trans. Power Electron.*, vol. 30, no. 1, pp. 4–17, Jan. 2015.

[3] S. Shao, A. J. Watson, J. C. Clare, and P. W. Wheeler, "Robustness analysis and experimental validation of a fault detection and isolation method for the modular multilevel converter," *IEEE Trans. Power Electron.*, vol. 31, no. 5, pp. 3794–3805, May 2016.

[4] N. Cherix, "Functional description and control design of modular multilevel converters: Towards energy storage applications for traction networks," Ph.D. dissertation, Lab. Ind. Electron., EPFL, Lausanne, Switzerland, 2015, doi: 10.5075/epfl-thesis-6479.

[5] B. Wu and M. Narimani, *High-Power Converters and AC Drives*. Hoboken, NJ, USA: Wiley, 2017.

[6] K. Sano and M. Takasaki, "A transformerless D-STATCOM based on a multivoltage cascade converter requiring no DC sources," *IEEE Trans. Power Electron.*, vol. 27, no. 6, pp. 2783–2795, Jun. 2012.

[7] R. Zeng, L. Xu, L. Yao, and B. W. Williams, "Design and operation of a hybrid modular multilevel converter," *IEEE Trans. Power Electron.*, vol. 30, no. 3, pp. 1137–1146, Mar. 2015.

[8] G. S. Konstantinou, M. Ciobotaru, and V. G. Agelidis, "Operation of a modular multilevel converter with selective harmonic elimination PWM," in *Proc. 8th Int. Conf. Power Electron. ECCE Asia*, May 2011, pp. 999–1004.

[9] A. El-Wakeel, M. Tawfik, and I. El-Arabawy, "A modified selective harmonic elimination method for balancing capacitor voltage in modular multilevel converter," in *Proc. IEEE Int. Conf. Environ. Electr. Eng. IEEE Ind. Commercial Power Syst. Eur. (EEEIC/I&CPS Eur.)*, Jun. 2017, pp. 1–6.

[10] A. Perez-Basante, S. Ceballos, G. Konstantinou, J. Pou, J. Andreu, and I. M. de Alegria, "(2N+1) selective harmonic elimination-PWM for modular multilevel converters: A generalized formulation and a circulating current control method," *IEEE Trans. Power Electron.*, vol. 33, no. 1, pp. 802–818, Jan. 2018.

[11] P. Enjeti and J. F. Lindsay, "Solving nonlinear equations of harmonic elimination PWM in power control," *Electron. Lett.*, vol. 23, no. 12, pp. 656–657, Jun. 1987.

[12] M. S. A. Dahidah, G. Konstantinou, and V. G. Agelidis, "A review of multilevel selective harmonic elimination PWM: Formulations, solving algorithms, implementation and applications," *IEEE Trans. Power Electron.*, vol. 30, no. 8, pp. 4091–4106, Aug. 2015.

[13] T.-J. Liang, R. M. O'Connell, and R. G. Hoft, "Inverter harmonic reduction using Walsh function harmonic elimination method," *IEEE Trans. Power Electron.*, vol. 12, no. 6, pp. 971–982, Nov. 1997.

[14] V. G. Agelidis, A. I. Balouktsis, and M. S. A. Dahidah, "A five-level symmetrically defined selective harmonic elimination PWM strategy: Analysis and experimental validation," *IEEE Trans. Power Electron.*, vol. 23, no. 1, pp. 19–26, Jan. 2008.

[15] H. Zhao, T. Jin, S. Wang, and L. Sun, "A real-time selective harmonic elimination based on a transient-free inner closed-loop control for cascaded multilevel inverters," *IEEE Trans. Power Electron.*, vol. 31, no. 2, pp. 1000–1014, Feb. 2016.

[16] F. Filho, L. M. Tolbert, Y. Cao, and B. Ozpineci, "Real-time selective harmonic minimization for multilevel inverters connected to solar panels using artificial neural network angle generation," *IEEE Trans. Ind. Appl.*, vol. 47, no. 5, pp. 2117–2124, Sep. 2011.

[17] S. S. Lee, B. Chu, N. R. N. Idris, H. H. Goh, and Y. E. Heng, "Switched-battery boost-multilevel inverter with GA optimized SHEPWM for standalone application," *IEEE Trans. Ind. Electron.*, vol. 63, no. 4, pp. 2133–2142, Apr. 2016.

[18] A. Routray, R. Kumar Singh, and R. Mahanty, "Harmonic minimization in three-phase hybrid cascaded multilevel inverter using modified particle swarm optimization," *IEEE Trans. Ind. Informat.*, vol. 15, no. 8, pp. 4407–4417, Aug. 2019.

[19] K. Haghdar, "Optimal DC source influence on selective harmonic elimination in multilevel inverters using teaching-learning-based optimization," *IEEE Trans. Ind. Electron.*, vol. 67, no. 2, pp. 942–949, Feb. 2020.

[20] M. H. Etesami, D. M. Vilathgamuwa, N. Ghasemi, and D. P. Jovanovic, "Enhanced metaheuristic methods for selective harmonic elimination technique," *IEEE Trans. Ind. Informat.*, vol. 14, no. 12, pp. 5210–5220, Dec. 2018.

[21] M. A. Memon, S. Mekhilef, M. Mubin, and M. Aamir, "Selective harmonic elimination in inverters using bio-inspired intelligent algorithms for renewable energy conversion applications: A review," *Renew. Sustain. Energy Rev.*, vol. 82, pp. 2235–2253, Feb. 2018.

[22] Z. Woo Geem, J. Hoon Kim, and G. V. Loganathan, "A new heuristic optimization algorithm: Harmony search," *Simulation*, vol. 76, no. 2, pp. 60–68, Feb. 2001.

[23] J. Yi, C.-H. Chu, C.-L. Kuo, X. Li, and L. Gao, "Optimized tool path planning for five-axis flank milling of ruled surfaces using geometric decomposition strategy and multi-population harmony search algorithm," *Appl. Soft Comput.*, vol. 73, pp. 547–561, Dec. 2018.

[24] J. Yi, L. Gao, X. Li, C. A. Shoemaker, and C. Lu, "An on-line variable-fidelity surrogate-assisted harmony search algorithm with multi-level screening strategy for expensive engineering design optimization," *Knowl.-Based Syst.*, vol. 170, pp. 1–19, Apr. 2019.

[25] O. Zarei, M. Fesanghary, B. Farshi, R. J. Saffar, and M. R. Razfar, "Optimization of multi-pass face-milling via harmony search algorithm," *J. Mater. Process. Technol.*, vol. 209, no. 5, pp. 2386–2392, Mar. 2009.

[26] R. S. Rao, S. V. L. Narasimham, M. R. Raju, and A. S. Rao, "Optimal network reconfiguration of large-scale distribution system using harmony search algorithm," *IEEE Trans. Power Syst.*, vol. 26, no. 3, pp. 1080–1088, Aug. 2011.

[27] K. Nekooei, M. M. Farsangi, H. Nezamabadi-Pour, and K. Y. Lee, "An improved multi-objective harmony search for optimal placement of DGs in distribution systems," *IEEE Trans. Smart Grid*, vol. 4, no. 1, pp. 557–567, Mar. 2013.

[28] M. N. Ambia, H. M. Hasanien, A. Al-Durra, and S. M. Muyeen, "Harmony search algorithm-based controller parameters optimization for a distributed-generation system," *IEEE Trans. Power Del.*, vol. 30, no. 1, pp. 246–255, Feb. 2015.

[29] E. E. Elattar, "Modified harmony search algorithm for combined economic emission dispatch of microgrid incorporating renewable sources," *Energy*, vol. 159, pp. 496–507, Sep. 2018.

[30] J. Yi, C. Lu, and G. Li, "A literature review on latest developments of harmony search and its applications to intelligent manufacturing," *Math. Biosci. Eng.*, vol. 16, no. 4, pp. 2086–2117, 2019.

[31] T. Zhang and Z. W. Geem, "Review of harmony search with respect to algorithm structure," *Swarm Evol. Comput.*, vol. 48, pp. 31–43, Aug. 2019.

[32] A. Askarzadeh, "Solving electrical power system problems by harmony search: A review," *Artif. Intell. Rev.*, vol. 47, no. 2, pp. 217–251, Feb. 2017.

[33] W. Fei, X. Ruan, and B. Wu, "A generalized formulation of quarter-wave symmetry SHE-PWM problems for multilevel inverters," *IEEE Trans. Power Electron.*, vol. 24, no. 7, pp. 1758–1766, Jul. 2009.

[34] R. Salehi, N. Farokhnia, M. Abedi, and S. H. Fathi, "Elimination of low order harmonics in multilevel inverters using genetic algorithm," *J. Power Electron.*, vol. 11, no. 2, pp. 132–139, Mar. 2011.

[35] M. Srndovic, A. Zhetessov, T. Alizadeh, Y. L. Familiant, G. Grandi, and A. Ruderman, "Simultaneous selective harmonic elimination and THD minimization for a single-phase multilevel inverter with staircase modulation," *IEEE Trans. Ind. Appl.*, vol. 54, no. 2, pp. 1532–1541, Mar. 2018.

[36] I. F II, *IEEE Recommended Practices and Requirements for Harmonic Control in Electrical Power Systems*, IEEE Ind. Appl. Soc., New York, NY, USA, 1993.

[37] Ö. Yeniay, "Penalty function methods for constrained optimization with genetic algorithms," *Math. Comput. Appl.*, vol. 10, no. 1, pp. 45–56, Apr. 2005.

[38] R. Storn and K. Price, "Differential evolution—A simple and efficient heuristic for global optimization over continuous spaces," *J. Global Optim.*, vol. 11, no. 4, pp. 341–359, 1997.

[39] Q.-K. Pan, P. N. Suganthan, M. F. Tasgetiren, and J. J. Liang, "A self-adaptive global best harmony search algorithm for continuous optimization problems," *Appl. Math. Comput.*, vol. 216, no. 3, pp. 830–848, Apr. 2010.

[40] P. Yadav, R. Kumar, S. K. Panda, and C. S. Chang, "An intelligent tuned harmony search algorithm for optimisation," *Inf. Sci.*, vol. 196, pp. 47–72, Aug. 2012.

[41] H.-B. Ouyang, L.-Q. Gao, S. Li, X.-Y. Kong, Q. Wang, and D.-X. Zou, "Improved harmony search algorithm: LHS," *Appl. Soft Comput.*, vol. 53, pp. 133–167, Apr. 2017.

[42] J. Yi, L. Gao, X. Li, and J. Gao, "An efficient modified harmony search algorithm with intersect mutation operator and cellular local search for continuous function optimization problems," *Appl. Intell.*, vol. 44, no. 3, pp. 725–753, Apr. 2016.

[43] P. I. Frazier, "A tutorial on Bayesian optimization," 2018, *arXiv:1807.02811*. [Online]. Available: http://arxiv.org/abs/1807.02811

YAYUN XIN received the B.S. degree in electrical engineering from the Wuhan University of Technology, Wuhan, China, in 2014. He is currently pursuing the Ph.D. degree with the School of Electrical and Electronic Engineering, Huazhong University of Science and Technology (HUST), Wuhan.

His research interests include power electronics and modular multilevel converters.

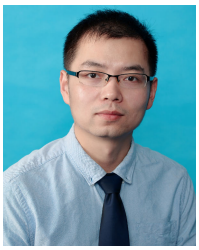

JIN YI received the B.S. and Ph.D. degrees in industrial engineering from the Huazhong University of Science and Technology (HUST), Wuhan, China, in 2012 and 2017, respectively.

He is currently a Research Fellow with the Environmental Research Institute, National University of Singapore. His research interest includes intelligent algorithms and their engineering applications.

KAI ZHANG received the B.S., M.S., and Ph.D. degrees from the Huazhong University of Science and Technology (HUST), Wuhan, China, in 1993, 1996, and 2001, respectively.

He joined HUST as an Assistant Lecturer, in 1996. He was a Visiting Scholar with the University of New Brunswick, Fredericton, NB, Canada, from 2004 to 2005. He was a Full Professor with HUST, in 2006. He is the author of more than 60 technical articles. His research interests include uninterruptible power systems, railway traction drives, modular multilevel converters, and electromagnetic compatibility techniques for power electronic systems.

CANFENG CHEN received the B.S. degree from Fuzhou University, Fuzhou, China, in 2017. He is currently pursuing the M.S. degree with the School of Electrical and Electronic Engineering, Huazhong University of Science and Technology, Wuhan, China.

His current research interests include modular multilevel converter and high-voltage direct current transmission.

JIAN XIONG received the B.S. degree from the East China Shipbuilding Institute, Zhenjiang, China, in 1993, and the M.S. and Ph.D. degrees from the Huazhong University of Science and Technology (HUST), Wuhan, China, in 1996 and 1999, respectively.

He joined HUST as a Lecturer, in 1999. He was an Associate Professor, in 2003. His current research interests include uninterruptible power systems, ac drives, switch-mode rectifiers, and STATCOMs and their related control techniques.